

Opto-Mechanical Design And Development of an Optodigital Confocal
Microscope

by

Vahid Pourreza Ghouschi

A Thesis Submitted to the
Graduate School of Science and Engineering
in Partial Fulfillment of the Requirements for
the Degree of

Master of Science

in

Optoelectronics & Photonics Engineering

Koç University

September, 2015

Graduate School of Sciences and Engineering

This is to certify that I have examined this copy of a master's thesis by

Vahid Pourreza Ghouschi

and have found that it is complete and satisfactory in all respects,
and that any and all revisions required by the final
examining committee have been made.

Committee Members:



Prof. Alper Kiraz



Asst. Prof. Alexandr Jonáš



Asst. Prof. Halil Bayraktar

Date: 29. 09. 2015

To my Parents...

Acknowledgments

Since, arriving at Koç University two years ago, I have gained academic gratification, and have made a lot of friendships. My special thanks and sincere appreciation goes to my advisor Prof. Alper Kiraz. I would not have succeeded in this journey without his invaluable help. I would like to thank Prof. Ali Serpengül, advisor of OSA chapter at Koç University, as he has had a positive impact on my academic life.

I deeply appreciate Dr. Alexandr Jonáš for being on my thesis committee and his remarks on my thesis. He is a meticulous and self-motivated person, and he greatly helped me in my thesis by suggesting many fruitful notes. I would like to thank Mr. Adnan Kurt who helped me a lot in this project. I also appreciate Dr. Muhsin Eralp for assisting me in Zemax simulations and Prof. Hakan Ürey for his valuable comments in ray optics. I am grateful to Dr. Halil Byraktar for being on my thesis committee and for his good feedback. I appreciate my friends at Koç University Dr. Reza Mokhtarzpour, Hadi Nozari, Dr. Mehdi Aas, Dr. Yasin Karadağ, Dr. Asuman Aşikğlu, Dr. Ahmet Erten, Mustafa Eryürek, Aziz Karasahin, Adil Mustafa and Selçuk Çakmak who created an environment that helped me to thrive in my work. I acknowledge all of my teachers from elementary school to high school especially my science teacher Mr. Hoseinzadeh, my mathematics teachers Mr. Masumkhah (may he rest in peace) and Mr. Golanazadeh (may he rest in peace) and my chemistry teacher Mr. Mohsen Ghofrani. I would like to express my gratitude to Graduate School of Science and Engineering of Koç University namely Elif Tüysüz, Emine Büyükdurmuş and Gözde Şirin for their endless help. lastely, I would like to sincerely thank my parents, my brothers and sisters who are my best friends and have always helped and motivated me. They have given me their love and support whenever I was in need, which I am truly grateful for.

This work was supported by The Scientific And Technological Research Council of Turkey (TÜBİTAK) grant No. 113F172.

ABSTRACT

Laser scanning confocal microscopy (LSCM) technique allows for obtaining high resolution, clear images of thin sections in a sample [1]. The power of a LSCM arises from exciting a very small region of the sample at a time and using a spatial filter, usually a pinhole, in front of the detector canceling the out of focus light. Then, 2D digital images can be constructed by scanning the desired field of view of the sample. Combining these images at the end, high resolution 3D images can be obtained [2,3].

Although, LSCM systems are widely used in biology, genetics, physics and other sciences, their high cost often requires central research facilities that hinders their wide use. The aim of this thesis was to develop a cost-efficient, compact and computer controlled LSCM using a Digital Micromirror Device (DMD) that eliminates the need for a scan lens and galvanometer. DMD chip is composed of micro mirrors, each of them functioning as a pinhole due to their rotation to two positions. High speed parallel scanning can be achieved by applying different patterns on the DMD chip that is located at the plane conjugate to the focal plane of the objective. Subsequently, by using a detector, digital images can be produced.

In this thesis, first a galvanometer mirror based LSCM was constructed. A program was developed to control the mirrors and gather data to form the images. Then a DMD-based optodigital LSCM was developed by using sequential patterns to scan the specimen. Optical and mechanical designs of the optical setups, optical alignment, optical simulation with Zemax , 3D CAD design with Solidworks and sampling with the program were accomplished.

ÖZETÇE

Lazer tarama eşodaklı mikroskobi (LSCM) tekniği bir örnekten alınmış ince bir kesitin yüksek çözünürlükte, net görüntülerini almayı sağlar [1]. Bu tekniğin gücü örnekte belirlenmiş küçük bölgelerin tek tek uyarılıp, genellikle iğne deliği yapısındaki uzamsal filtre detektörün önüne konumlandırılıp, bulanık ışığın elimine edilmesine dayanır. Daha sonra da, örneğin istenilen bölümü taranarak dijital 2 boyutlu resimleri elde edilir. Bu 2 boyutlu resimler de sonradan bir araya getirilerek, cismin yüksek çözünürlüklü 3 boyutlu resimleri elde edilebilir [2,3].

Her ne kadar LSCM sistemleri biyoloji, genetik, fizik ve diğer bilim dallarında geniş kullanım alanı bulsalar da, yüksek maliyetleri genellikle merkezi araştırma laboratuvarlarının karşılayabileceği bir güçlüktür bu da yaygın olarak kullanımlarının önüne geçer. Bu tezin hedefi Dijital Mikroayna Cihaz (DMD) kullanılarak lens ve galvanometreye duyulan ihtiyacı ortadan kaldırarak uygun maliyetli, kompakt ve bilgisayar tabanlı LSCM geliştirmektir. DMD çipi mikro aynalardan oluşur ve bu aynaları her biri iki pozisyona rotasyonlarından dolayı iğne deliği gibi işler. Yüksek hızlı paralel tarama objektifin eşlenik düzlemiyle odağı arasında yer alan DMD çipinin üzerine farklı desenlerin uygulanmasıyla elde edilebilir. Sonrasında da, detektör yardımıyla dijital görüntüler oluşturulabilir.

Bu tezde ilk olarak, LSCM tabanlı galvanometre yapıldı. Görüntülerin oluşturulması için aynaları kontrol eden ve veri toplayan program geliştirildi. Daha sonra da örneği tarayabilmek için sıralı desenler kullanılarak DMD tabanlı opto-dijital LSCM geliştirildi. Optik ve mekanik tasarım için gerekli olan optik düzenlemeler, yerleştirme ve simülasyon Zemax ile, 3 boyutlu CAD tasarımı Solidworks ile ve örneklemeler de program aracılığıyla gerçekleştirildi.

Contents

1	Introduction	1
1.1	Light Microscopy	1
1.2	Finite Tube Length Microscope	4
1.3	Microscopes with infinity corrected objectives	4
1.4	Numerical Aperture (NA)	6
1.5	Magnification	7
1.6	Resolution in Microscopy	8
1.7	Illumination Methods	11
1.8	Field of View (FOV),Field Stop and Field Number	12
1.9	Depth of Focus And Depth of Field	13
2	Confocal Microscopy	15
2.1	Introduction to Confocal Microscopy	15
2.2	Point Scanning Confocal Microscopy	16
2.3	Spinning Disk Confocal Microscopy	18
2.4	Fluorescece Microscopy	19
2.5	Multiphoton microscopy	20
2.6	Light Sources in Confocal Microscopy	22
2.7	Resolution In Confocal Microscopy	22
2.8	Detectors For Confocal Microscopy	23
2.9	Limitation of Laser Scanning Confocal Microscopy	24
3	Opto-Mechanical development of a Laser Scanning Confocal Microscope (LSCM)	26
3.1	Optical Setup	26
3.1.1	Laser Source	26
3.1.2	PMT	26

3.1.3	Galvanometer Mirror	27
3.1.4	Scan Lens	28
3.1.5	Objective Lens	32
3.1.6	Microscope Body	32
3.1.7	CMOS Camera	33
3.1.8	Filters and Dichroic Mirrors	33
3.2	Optical Alignment	34
3.3	How LSCM Setup Works:	36
3.4	3D CAD Drawings of The LSCM Setup	38
3.5	Control and Data Acquisition Unit	40
3.6	Confocal Software	42
3.7	Simulations With Zemax	44
3.7.1	Simulation Procedure	45
3.7.2	3D Diagram of The Setup	46
3.7.3	Spot Size Diagram	47
3.7.4	Footprint Diagram	48
3.7.5	MTF Diagram	48
3.8	Spot Size Analysis of LSCM setup	50
3.9	Scanning Results of The LSCM Setup	53
4	Digital Micromirror Device (DMD) Based Microscope	54
4.1	What is a Digital Micromirror device (DMD)?	54
4.2	DLP LightCrafter Evaluation Module (EVM)	55
4.3	Developing a DMD Based Microscope	57
4.4	Optical Alignment	58
4.5	How The DMD Based Setup Works?	60
4.6	DLP Graphic User Interface (GUI)	62
4.7	Scanning Results of the DMD Based Setup	64
4.7.1	Projection of the Images and pattern sequences by the use of DMD into focal plane of the objective	64
4.7.2	Movie projection	65

5 Appendix 66

Bibliography 68

Index 72

Glossary 72

List of Figures

1.1	The first compound microscope [4], built by Zacharias Janssen.	2
1.2	Schematic of a microscope [5]. The objective lens forms a real magnified image of a close sample, then eyepiece further magnifies this image and produce a virtual image. This image is larger and does not need to fit inside the optical tube of the microscope.	4
1.3	This figures shows a microscope [6] with infinity corrected objective. A tube lens is used after the objective to form the intermediate image.	5
1.4	Numerical Aperture for the objective of a microscope [7]	6
1.5	Airy disk diameter in diffraction parrrten.	9
1.6	This figures [8] indicates how two points are not resolvable (a), barely resolvable(Sparrow limit(b)), resolvable (Rayleigh limit (c)) and clearly resolvable(d).	10
1.7	In this figure α is the half of angular field of view [9].	12
1.8	Spatial field of view on an object [10].	12
2.1	Schematic a of a confocal microscope [1] - Light after passing through the first pinhole (A) and the condenser lens (C) has and image on the sample (S). Then by employing an objective lens (o), a point on the sample (D) is imaged to the second pinhole before the detector (B). The advantage of the second pinhole is, it excludes the light from out of focus points (E).	16
2.2	Schemtic of a Laser scanning confocal microscope [11].	17
2.3	Configuration of a Yokogawa Disk-Scanning Confocal System [12].	18
2.4	Spectrum of the excitation and emission beam [13]. Stokes shift displays how emission peak was shifted toward a larger wavelength.	19
2.5	Schematics of a fluorescence microscope setup [13]	20
2.6	Schematic of two-photon excitation [13]. Two photons that strike the fluorophore absorbed and the higher energy photon is emitted.	21
2.7	Configuration of a typical PMT with array of dynodes. [13]	24
3.1	Spectral response of the PMT (used in our experimental setup, indicated with the red line) [14].	27
3.2	Image Of the PMT with pinhole, cage system and lens.	28
3.3	Galvanometer Scanning Mirrors :The sample is scanned in X and Y axis by employing two scanning mirrors.	29

3.4	Image plane of a Spherical lens (a), a flat-field scanning lens (b) and a f-theta scanning lens [15].	29
3.5	Telecentric condition in a scan lens [16].	30
3.6	Optimal distances for scanning configuration for CLS-SL Scan Lens [15].	31
3.7	Nikon MRP05422 objective specifications.	32
3.8	1- Laser source ($\lambda=532$ nm), 2- Continuously variable, metallic neutral density (ND) filter for altering the intensity, 3- ND filter, 4-Plano-convex lens $f=200$ mm, 5-Mirror, 6-Plano-convex lens $f=50$ mm, 7- Plano-convex lens $f=100$ mm, 8- Mirror, 9- Dichroic Mirror 10- Diaphragm, 11-Galvanometer (Scanning Mirror), 12- Scan Lens $F=70$ mm, 13- Beam Splitter, 14- A tube lens and microscope objective (40X, 2.1mm working distance, $NA=0.55$), 15-Camera for obtaining real time images, 16- Convex lens $F=50$ mm, 17- Photo Multiplier Tube (PMT)	36
3.9	Schematics of some parts designed in solidworks.	39
3.10	Schematics of 3D design of the microscope	39
3.11	Top view of 3D drawing of the optical setup.	40
3.12	Side view of 3D drawing of the optical setup.	40
3.13	Flowchart of the LSCM system	41
3.14	Control and data acquisition unit.	42
3.15	Confocal program graphical user interface.	43
3.16	Scanning values are entered to the system from this window.	44
3.17	Three configurations of the scanning mirror that represents three scanning angles. . .	46
3.18	3D diagram of the LSCM system in Zemax	47
3.19	The standard spot diagram at image plane for the three scanning configurations, 3, 0 and -3 degrees.	47
3.20	The footprint Diagram at image plane for the 3, 0 and -3 degrees scan angles	48
3.21	FFT MTF diagram for the first and third configurations, 3 and -3 degrees scan angle. .	49
3.22	FFT MTF diagram for the second configuration, zero degree scan angle.	49
3.23	Diffraction limit of the system occurs at 2200 spatial frequency.	50
3.24	3D surface plot of the minimum spot of the LSCM setup.	51
3.25	Minimum spot of the LSCM setup.	51
3.26	Minimum spot of the LSCM setup.	52
3.27	sample (left) and the image obtained by the LSCM (right)	53
4.1	Two operational states of the DMD chip. [17].	54

4.2	Image of the DMD mirrors with SEM microscope [18]	55
4.3	Mirror arrays in DLP3000 DMD chip. [19]	56
4.4	Inside of the light engine of the LightCrafter EVM (top view) [20].	56
4.5	Inside of the light engine of the LightCrafter EVM (bottom view) [20].	57
4.6	Schematics of the DMD based optical setup	58
4.7	DMD based microscope optical setup: 1.Laser, 2.Mirror 3.Mirror 4.Plano-convex lens f=50 mm 5.Variable ND filter, 6.Plano-convex lens f=200 mm 7.Mirror 8.Diaphragm, 9.DMD 10.Tube lens and objective, 11.Camera.	59
4.8	DLP chip and its holder.	59
4.9	The side view of the DMD based microscope optical setup.	62
4.10	Graphic user interface of the DLP LightCrafter EVM.	63
4.11	A uploaded and the projected pattern on the focal plane of the objective.	64
4.12	Original pattern and projected pattern of "Kiraz Lab" on the focal plane of the objective.	65

List of Tables

1.1	Microscope manufacturers and corresponding focal length for the tube lens. . .	5
1.2	Magnification, Numerical Apertures, Effective Focal Length and Working Distance for typical microscope objectives [7].	7
3.1	Specification of CLS-SL Scan Lens(FN means field number) [15].	31
3.2	Specification of DCC1240M Camera [21].	33
5.1	General System Data for LSCM system simulated in Zemax.	67

CHAPTER 1

Introduction

1.1 Light Microscopy

Human being has been interested in microscopy from ancient time. Microscopy refers to a technique used to visualize tiny objects that cannot be seen by the human's naked eye. The simplest microscope can be formed by a single lens when the object is located at its focal length. The first compound microscope, (see figure 1.1) was built by Zacharias Janssen around 1595 [22]. The term compound is used since two or more lenses are employed to construct a microscope. In 1609, the famous Italian physicist, Galileo Galilei, designed a new microscope with higher magnification by employing a biconvex and a concave lens. Fifty six years later a British scientist Robert Hooke, published his observations of various objects in his book, *Micrographia*. His observations of tiny organisms and his excellent schematics had a deep effect in biology. He was one of the first people in the history, who saw cells [23]. Later, Antonie van Leeuwenhoek, a Dutch microscopist, built many lenses and employed them in microscopes. He was the first man in the history to see the bacteria in 1683 [24]. In 1873 Ernst Abbe proposed his famous diffraction limit formula and founded the base of the modern microscopy [25]. Subsequently, German scientist Ernst Ruska, invented the first electron microscope in 1931. Finally, in 1957 Marvin Minsky invented confocal microscopy at MIT University.

Today there are state-of-art microscopes and many methods of microscopy are used in different fields. The three primary branches in microscopy are electron, Optical and Scanning probe microscopy. In this thesis, I will discuss optical microscopy. Then in the second chapter Laser Scanning Confocal Microscopy will be discussed in detail. Fundamental of light microscopy

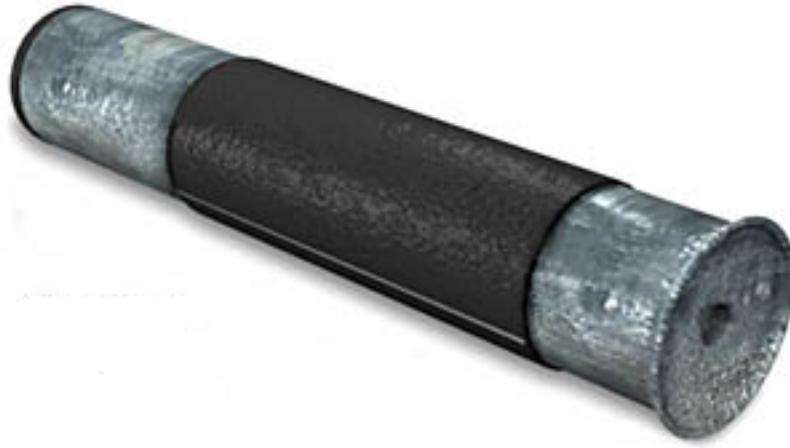


Figure 1.1: The first compound microscope [4], built by Zacharias Janssen.

were discussed in details in "Fundamentals of Light Microscopy and Electronic Imaging" [25], "Field Guide to Microscopy" [5], "Optical Design of Microscopes" [26], and various application in "Handbook of Microscopy" [27]. There are various techniques in light microscopy and some common methods are:

Dark field microscopy is a microscopy method to image objects that are not clearly visible with conventional bright field microscopy. It applies a dark field stop in front of the condenser to eliminate the center of cone of light. Therefore, the transmitted beam does not enter the objective and just scattered light passes through the objective lens. Hence, the contrast of the images is increased. Dark field microscopy is a convenient method for imaging the unstained sample. However, the major drawback is, very low intensity of the image. Therefore, the intensity of the source should be increased that may result in photo bleaching.

Phase contrast microscopy is a technique specially used in biology for detecting transparent specimen, invented in 1934 by a Dutch physicist Frits Zernike [28,29]. Although, light intensity and phase after passing through the specimen is changed, however, human eye and optical cameras are just sensitive to intensity changes. By employing phase contrast microscopy phase shifts can be transferred into intensity changes, therefore, transparent samples that are invisible with bright field microscopy can be detected [25] with phase contrast microscopy. On the other hand phase contrast microscopy is not suitable for thick specimen.

Confocal Microscopy refers to a method in microscopy that employs a point source for illuminating the sample. A pinhole is used in the confocal point for detection. This pinhole rejects the out of focus light and enhances the contrast and image quality. Confocal microscopy is used in biological imaging specially for thick specimen. Confocal microscopy is discussed in chapter two in great details.

fluorescence microscopy is another technique in that a fluorescence sample is excited with a special frequency. Then, sample emits a light with a larger frequency. By using a dichroic mirror for splitting the excitation and emission light, fluorescence images can be obtained. For enhancing the contrast, fluorescence microscopy is used in with confocal microscopy. living cells, For example, can be genetically altered to carry the Green fluorescence Protein (GFP) and then detected by the fluorescence light from the cells [13].

Multiphoton (two-photon) microscopy describes a technique in which two photon with enough energy to excite the fluorophore transfer their energy to the fluorophore and excite it. Then a beam with different energy is emitted. Note that, the excitation beams each has lower energy than emission beam. By employing a dichroic mirror, excitation and emission beams can be separated. Multiphoton microscopy has better image contrast than fluorescence microscopy and is discussed in the next chapter.

Differential Interference Contrast(DIC) microscopy is a method for enhancing image contrast of the unstained samples. DIC microscopy is polarizing microscopy technique in which polarized beam is separated into two beams by employing a DIC prism. Later, these beams after passing through the sample and the objective are combined by applying another DIC prism at the back focal plane of the objective. Then, by employing a compensator and an analyzer images can be obtained with higher contrast. DIC microscopes provide 3D images relative to phase contrast images, however, phase contrast images have higher contrast.

As it was discussed each sample needs its own appropriate method for microscopy and illumination techniques are very important in optical microscopy and can deeply affect the final image. Various methods of microscopy were discussed in this paper [30].

1.2 Finite Tube Length Microscope

A simple schematic of a microscope that is composed of an objective lens and an eyepiece was illustrated in the figure 1.2. For image formation the sample is placed very close to objective focal plane and rays emerging from the sample after passing through the objective form a magnified intermediate real image very close to the front focal length of the eyepiece. This real image serves as an object, then eyepiece produces a final magnified virtual image at infinity. In order to see this virtual image, we need another optical instrument(usually observer's eye) to convert it to a real image.

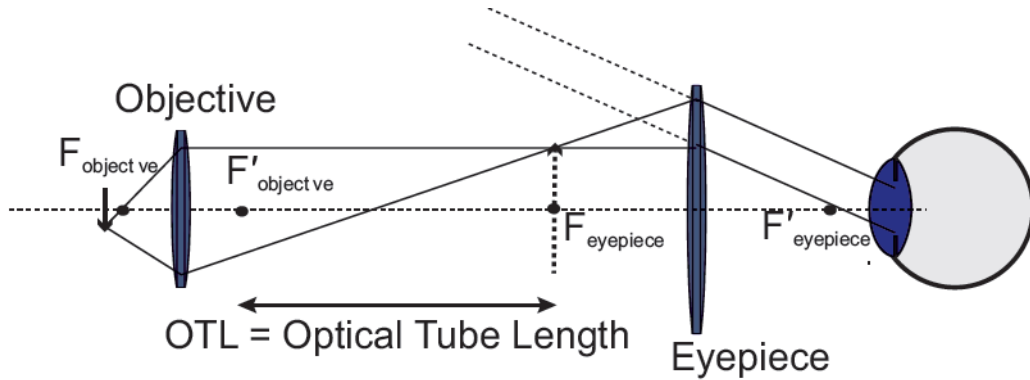


Figure 1.2: Schematic of a microscope [5]. The objective lens forms a real magnified image of a close sample, then eyepiece further magnifies this image and produce a virtual image. This image is larger and does not need to fit inside the optical tube of the microscope.

Optical tube length (OTL) the distance from the objective's back focal length to the front focal length of the eyepiece. By suggestion of Royal Microscopical Society (RMS), the standard OTL was set to 160 mm [6,31]. Nowadays, most optical microscopes have infinite tube length that make it very convenient to use filters and optical components between objective and eyepiece. Infinite tube length microscopes is discussed in the next section.

1.3 Microscopes with infinity corrected objectives

State-of-the-art microscopes usually utilize infinity corrected objectives that create collimated beam at the exit pupil of the objective. The advantage of these systems over finite tube length

systems is that optical components such as beam splitters, filters, prisms and etc. for different applications can easily be added to the optical path of the microscope. The following figure displays the optical schematic of a microscopes that employs an infinity corrected objective:

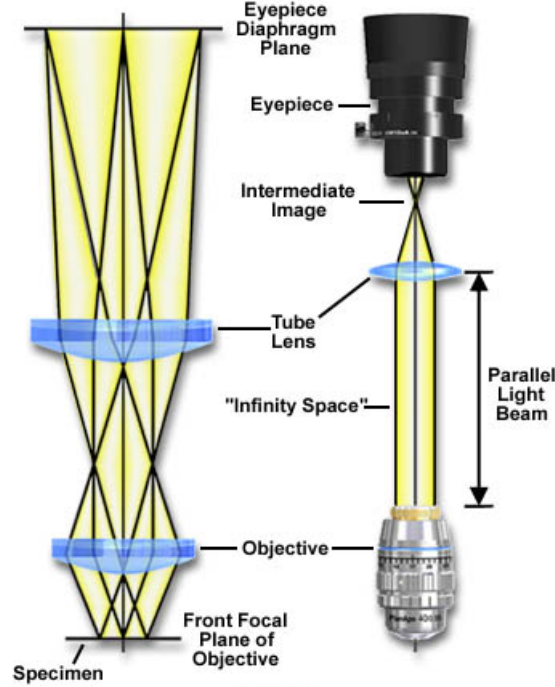


Figure 1.3: This figures shows a microscope [6] with infinity corrected objective. A tube lens is used after the objective to form the intermediate image.

As shown in the figure 1.3 light diffracted from the sample after passing through the objective is collimated. This parallel beam passes through a tube lens that forms an intermediate real image at the back focal plane of the lens. This intermediate real image serves as object for the eyepiece, reimaged with an eyepiece to see the final image by human eye. Table 1.1 shows different manufacturers use various focal length tube lenses [5].

Manufacturer	Focal length for Tube Lens
Nikon	200 mm
Zeiss	164.5 mm
Olympus	180 mm
Leica	200 mm

Table 1.1: Microscope manufacturers and corresponding focal length for the tube lens.

1.4 Numerical Aperture (NA)

Numerical aperture (NA) is a very important concept in microscopy and fiber optics. Numerical Aperture defines the acceptance angle of rays from the object space, passing through the system [5]. Shown in the equation 1.1, numerical aperture is a fundamental concept since it affects the lateral and axial resolution of the system.

$$NA = n \sin \theta \quad (1.1)$$

NA of an objective lens depends on the refractive index of the object space medium and sinus of half of angle of the cone of rays emerging from object into the objective lens. In other words NA of an objective, specifies the ability of the objective to collect light from the sample. NA value of an objective is depends on how well the object is corrected for different optical aberrations.

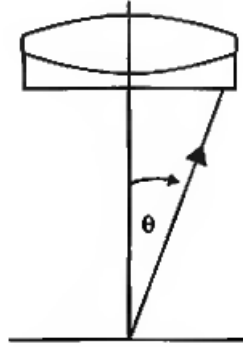


Figure 1.4: Numerical Aperture for the objective of a microscope [7]

Shown in figure 1.4 NA is the acceptance angle of the objective of a microscope. Later we will see how the resolution of the microscope depends on the NA of the objective. The following table shows the NA of some typical microscope objectives and their corresponding magnification (Mag), Effective Focal Length (EFL) and Working Distances (working distance is the distance from the front edge of the objective to its front focal plane):

Mag	NA	EFL(mm)	WD(mm)
5x	0.12	24.8	27.4
10x	0.25	14.6	7.3
20x	0.54	8.4	1.6
40x	0.60	4.6	0.8

Table 1.2: Magnification, Numerical Apertures, Effective Focal Length and Working Distance for typical microscope objectives [7].

Another important concept in an optical systems that is an alternative for NA is F-Number (f/number, f/# or focal ratio). For a infinite conjugate f-number is:

$$F/\# = \frac{\text{focal length}}{\text{clear aperture diameter of the lens}} = \frac{1}{2NA} \quad (1.2)$$

Where NA is the numerical aperture. This definition is useful for the infinite conjugate and photography when the object is far from the lens [32]. However in optical design , working f-number is used when object is close to the lens. The working $F/\#$ is defined as the image distance over Entrance Pupil Diameter (EPD). Working f-number and f-number are related to each other by the following formula in which m is the magnification of the system [8]:

$$F/\#_{Working} = F/\#(1 + |m|) \quad (1.3)$$

Many of the optical properties such as: size of the diffraction limited image, depth of focus, aberration and .etc are related to f-number. On the other hand, f-number is the ability of the optical system to gather light and the smaller f-number the brighter image will be. The irradiance of the image is inversely proportional to the square of the f-number. This means if f-number increased by the factor of two then irradiance will decrease by the factor of four.

1.5 Magnification

Magnification is the ability of the optical system to provide magnified images of the objects.

There are three kinds of magnification: Lateral(transverse, radial or linear) magnification, Angular magnification and longitudinal(Axial) magnification. Axial magnification will be discussed later. Lateral magnification is defined as the ratio of the image height to the object height or alternatively image distance to the object distance from the lens. The ratio of the angle that image emanate to the object angle is called angular magnification. The linear magnification of the objective is $M_o = \frac{L}{f_o}$, in which L is the tube length of the microscope and f_o is the front focal length of the objective. For an infinity corrected objective magnification is equal to the ratio of the "focal length of the tube lens" to the front focal length of the objective. The angular magnification of the eyepiece is $M_e = \frac{250mm}{f_e}$ where f_e is the eyepiece focal length and 250 mm is coming from the near distance of the human eye. The total magnification of a microscope is defined as:

$$M_{Total} = M_e * M_o = \frac{250mm}{f_e} * \frac{L}{f_o} \quad (1.4)$$

The minimum magnification of a microscope considering which wavelength is used is between 250NA to 500NA range [5]. For convenient sampling, 1000NA magnification is desired. The magnification that is larger than 1000 NA, increases the image size but does not provide more details and it is called empty magnification. For larger magnifications the image will have lower contrast and on the other hand the resolution would be the same.

1.6 Resolution in Microscopy

Resolution or resolving power of an optical system refers to the minimum resolvable distance between two close luminous points that can still be distinguished as two separated points. The resolution is the most critical criteria to indicate how good is a microscope in detecting tiny objects.

Image of a sample in cover slip of the microscope is visible because of the diffraction. If a point source is focused by a singlet on the screen, 2D diffraction pattern will be visible on the

Screen. The central bright spot of the diffraction pattern is called Airy disk and was named after George Biddle Airy, who first calculated the radius Airy Disk (figure 1.5).

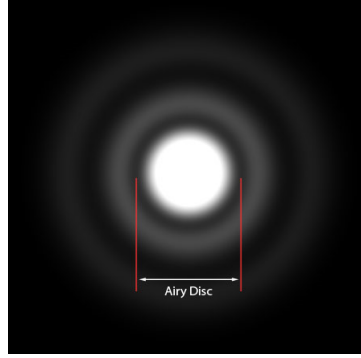


Figure 1.5: Airy disk diameter in diffraction pattern.

The radius of the Airy disk is important since it has 84% of the intensity of the light and can be calculated as

$$d = 1.22 \frac{f\lambda}{D} \quad (1.5)$$

In which f is the focal length of the lens, D is the diameter of the lens and λ is the wavelength of the light. In 1883 German scientist Ernst Abbe proposed a formula for resolution and founded the bases of the modern microscopy [33]. Due to Abbe's formula the resolution of an optical system is limited by diffraction and can be calculated by 1.6 equation.

$$d_{min} = \frac{\lambda}{2\sin\theta} \quad (1.6)$$

In equation 1.6 θ is half angle of the angular aperture of the lens and λ is the wave length of the light. As shown in equation 1.6 the highest possible resolution for light microscopy is 200 nm.

There are various definitions for the resolution such as Rayleigh criteria or Sparrow criteria. The most common definition for resolution in microscopy is Rayleigh criterion that describes the minimum resolvable distance of two point sources as the situation in which the central

maximum of diffraction image of one point source (Airy disk) just overlaps with the first radial minimum of the other point source [8]. The Rayleigh resolution can be calculated from equation 1.7 in which, λ is the wavelength, NA is the numerical aperture of the objective.

$$d_{Rayleigh} = \frac{0.61\lambda}{NA} \quad (1.7)$$

This expression suggests that the resolution can be improved by either using shorter wavelength or water or oil immersion objectives with higher NA (the highest theoretical value of NA is 1.51 [34]).

$$d_{Sparrow} = \frac{0.5\lambda}{NA} \quad (1.8)$$

Equation 1.8 shows another criterion that was introduced for calculating the resolution called Sparrow criteria. Sparrow resolution is 20 percent smaller compared to Rayleigh resolution limit [8].

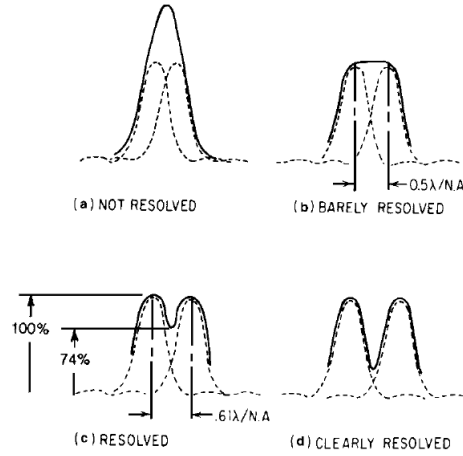


Figure 1.6: This figures [8] indicates how two points are not resolvable (a), barely resolvable (Sparrow limit (b)), resolvable (Rayleigh limit (c)) and clearly resolvable (d).

Figure 1.6 illustrates different resolution definition and correspondent diffraction patterns.

1.7 Illumination Methods

There are two major illumination methods: transmitted illumination and epi-illumination (which is also called reflection microscopy or metallurgical microscopy). In transmitted microscopy light from the source passes through the sample and enters the objective. Epi-illumination describes an illumination method in which light after passing an objective strikes a sample. Afterwards, the illumination light passes through the same objective and by using an eyepiece or camera images can be obtained. Epi-illumination is widely used in confocal microscopy, fluorescence microscopy and multiphoton microscopy.

One of the important factors in microscopy that impacts on the image quality and contrast is how to illuminate the sample. August Köhler in 1893 [26] invented a method that is called Köhler illumination for illuminating the sample. In his method sample is illuminated uniformly and brightly even though the light source is not uniform. Köhler illumination system consists of a source, a collector lens, a field aperture (location of the field stop), a condenser diaphragm and a condenser lens. This system is configured in such a way that image of the source created by the collector lens completely fills the condenser aperture located in the condenser front focal plane. Consequently, the sample is uniformly illuminated by a set of plane waves that originate from different points in the condenser front focal plane and propagate at different angles with respect to the optical axis of the microscope. Note that in the Köhler illumination the field stop, sample and intermediate image are at conjugate planes. Köhler illumination can be used with both transmitted or epi-illumination.

1.8 Field of View (FOV), Field Stop and Field Number

Field Of View (FOV) is the portion of the object that can be viewed or imaged by an optical system. FOV can be represented in two ways, angular field of view or spatial field of view. Angular field of view determines the angle that emanate from the object space and can be seen or imaged (see figure 1.7). Spatial Field of view determines the dimension of the object that can be imaged (see figure 1.8).

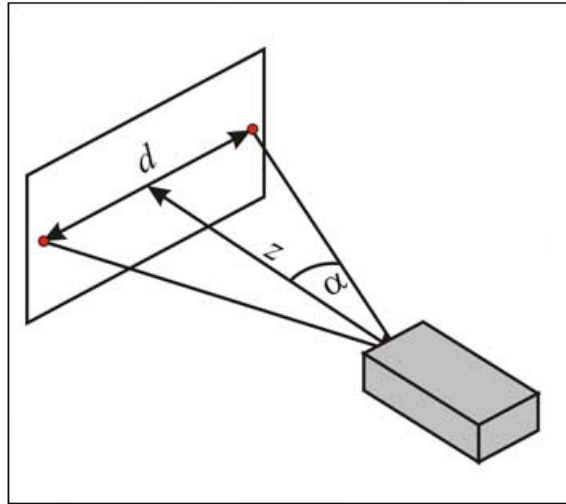


Figure 1.7: In this figure α is the half of angular field of view [9].

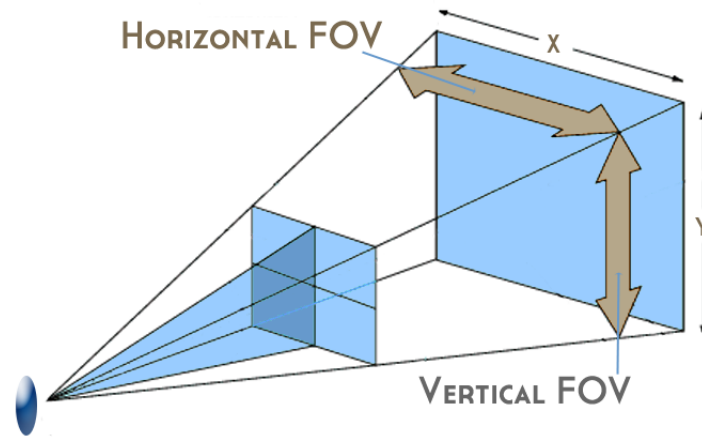


Figure 1.8: Spatial field of view on an object [10].

Field stop of an optical system controls the angular and spatial field of view in an optical system [8]. For instance in a house, a window represents the field stop. In principle when a sensor is used for imaging, the dimension of the sensor is the field stop in the optical system. However, if there is an intermediate image (in the case an eyepiece is used), its location represents the field stop of the system. The diameter of the field stop for an optical component, for example an eyepiece, is called field of view number or field number. Field number is normally engraved on eyepiece of the microscope that can be used in equation 1.9 to determine the field of view.

$$FOV = \frac{\text{Field Number Of Eyepiece}}{\text{Magnification}_{objective}} \quad (1.9)$$

If a detector is used for obtaining image in the microscope the dimension of the sensor chip over magnification indicates the FOV (equation 1.10) [35].

$$FOV = \frac{\text{Sensor Dimension Of The Detector}}{\text{Magnification}_{objective}} \quad (1.10)$$

1.9 Depth of Focus And Depth of Field

Depth of field refers to axial shift of the object for which image stays in focus. The corresponding axial shift for the image is called Depth Of focus. Depth of field determines the axial resolution of a microscope. For a diffraction limited optical system, depth of field can be calculated by equation 1.11. [25]. For a microscope the total depth of field is calculated by equation 1.12 :

$$\text{DepthOfField} = \frac{n\lambda}{NA_{obj}^2} = 4n\lambda f\#^2 \quad (1.11)$$

$$\text{DepthOfField}_{total} = \frac{n\lambda}{NA_{obj}^2} + \frac{n * e}{M_{obj} * NA_{obj}} \quad (1.12)$$

In equations 1.12 n is the refractive index of the medium between objective and sample, NA is the numerical aperture of the objective, M is magnification of the objective, e is the smallest resolvable distance by the camera(pixel size) and λ is the applied wavelength. Depth of field is used to determine the axial resolution of the microscope and also is a substantial factor in photography to take sharp images. For a larger diaphragms (higher NA or lower f-number) DOF is shallow. Sometimes depth of focus is also important as it tells, in what range the camera sensor can move and still obtains sharp images. By increasing the magnification depth of field is decreased while depth of focus is increased.

CHAPTER 2

Confocal Microscopy

2.1 Introduction to Confocal Microscopy

Confocal microscopy was first invented by M. Minsky in 1957 [1] and as time passed it became a popular microscopy technique specially in biological imaging. Confocal microscopy has some advantages over conventional wide field microscopy such as: high contrast images, higher lateral resolution, and obtaining clear images from different thin sections of the specimen. Therefore, confocal microscopy is very useful in scanning thick samples. Because of the limited depth of focus, three dimensional images can be created from different images of thin sections of the sample, if a z axis scanner is attached to the microscope. Confocal microscopy employs point illumination for scanning a small desired field of view in the object plane. For image formation a spatial filter, usually a pinhole, is used that is conjugate to the object plane and prevents the out of focus beam from reaching the detector. There are some good references on confocal microscopy such as "Handbook of Biological Confocal Microscopy" by J. B. Pawley [1], R. H. Webb review paper on confocal microscopy [3] or "Confocal microscopy method and protocols" by Stephen W. Paddock [36]. For further references on light microscopy and confocal microscopy reader can see bibliography.

The principle of the confocal imaging is illuminating sample by a point source, or alternatively putting a pinhole in front of a wide source, and employing another pinhole conjugate to the sample. The second pinhole limits the field of view and cancels out of focus light. Most confocal imaging systems rather than using a condenser lens for illuminating the object use epi-illumination in which objective serves both as condenser and objective lens. Confocal

microscopy schematic was depicted in in the following image:

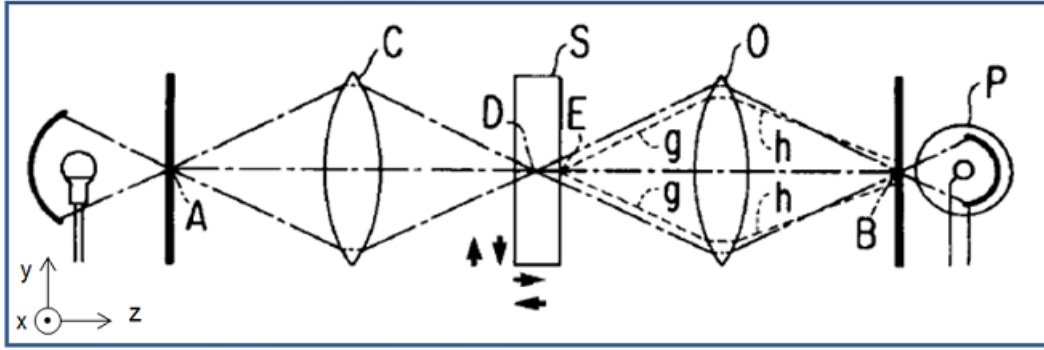


Figure 2.1: Schematic a of a confocal microscope [1] - Light after passing through the first pinhole (A) and the condenser lens (C) has and image on the sample (S). Then by employing an objective lens (o), a point on the sample (D) is imaged to the second pinhole before the detector (B). The advantage of the second pinhole is, it excludes the light from out of focus points (E).

Figure 2.1, displays confocal imaging in transmitted illumination. Pinhole diameter should be selected small enough to prevent higher order diffrational rings and just accept the Airy disk of the image. In confocal microscopy the desired field of view on the sample is scanned by different methods in tangential (X-Y) plane. For obtaining image form different sections of the specimen sample is moved in Sagittal (axial) plane.

2.2 Point Scanning Confocal Microscopy

In this practice on point of the sample is scanned then it moves to another point until the whole field of view is scanned. This process is possible by either moving the sample in tangential plane or employing two galvanometer mirrors. The fast axis galvanometer mirror is scans in X direction and slow axis galvanometer scans in Y axis. In point scanning confocal microscopy the maximum lateral resolution can be achieved. The main disadvantage of this method is low sampling rate.

In early years of 1970's Egger developed a confocal microscope with a laser source [1]. In his microscope the objective was moved to scan the sample. In later years Sheppard (1978)

and Wilson (1980) developed an epi-illumination stage scanning confocal microscope with a Photomultiplier Tube (PMT) as a detector and a modern scanning stage that could be moved in three dimensions [1]. This microscope was a fascinating invention since it could provide clean images of the optical sections of Integrated Circuits (IC). As time passed, laser scanning confocal microscope was implemented for biological imaging.

During this period various researchers from different countries contributed in the improvement of LSCM and finally microscope manufacturers like Zeiss, Olympus and others produced the commercial laser scanning confocal microscopes. These precious devices could scan biological samples with high NA objectives, saved the image in their memory and constructed the 3D view of the sample. In modern LSCM systems the specimen is not moved and scanning mirrors are used for beam steering in two dimensions. Additionally, they employ epi-illumination for illuminating the specimen.

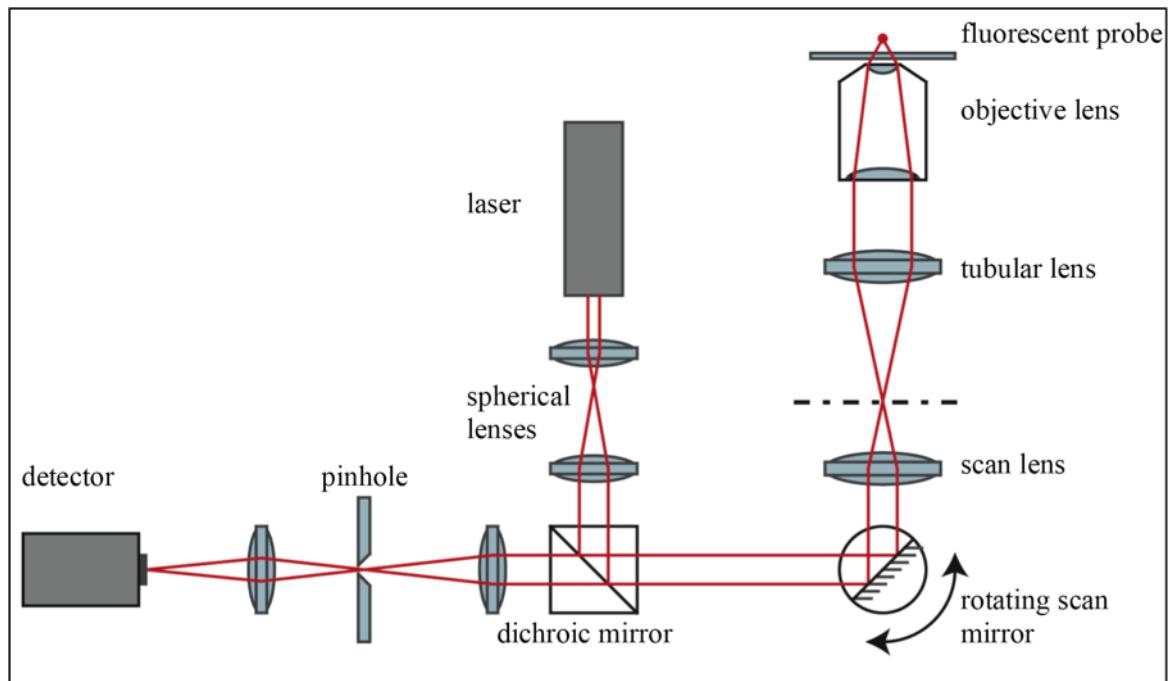


Figure 2.2: Schematic of a Laser scanning confocal microscope [11].

2.3 Spinning Disk Confocal Microscopy

Scanning a sample using a wheel with raster pattern was first proposed by German scientist Paul Nipkow in 1884. In 1967 Mojmir Petrán built a tandem-scanning-confocal microscope. In this method light after passing a spinning disk with holes illuminated the sample. The beams transmitted through each hole of the spinning disk and, subsequently, focused on the specimen by the objective lens were reflected from the specimen and after passing the same objective they were imaged on the Nipkow disk. Each hole on the Nipkow disk acted like a pinhole just like a confocal microscope and rejected the out of focus light. Later other version of the spinning disk microscope was built by Gordon Kino at Stanford University [1].

The spinning disk method unlike the point scanning confocal microscope worked as a parallel scanning technique with 100 to 1000 time higher speed. The major drawback of this method was gathering very low (1% or 2%) portion of the illumination light by the detector. Modern Spinning disk confocal microscopes, Yokogawa Disk-Scanning Confocal System (figure 2.3), for example employ micro-lenses on the first disk to resolve the issue.

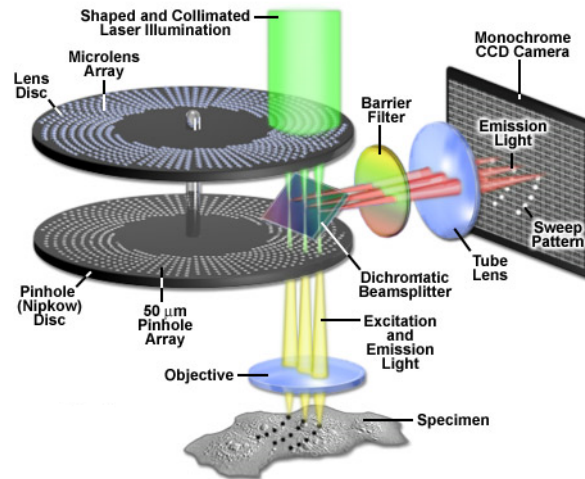


Figure 2.3: Configuration of a Yokogawa Disk-Scanning Confocal System [12].

2.4 Fluorescence Microscopy

To improve the image contrast and obtaining high quality images, confocal microscopy is commonly used with fluorescence microscopy. In fluorescence microscopy illumination light with a special wavelength is absorbed by the sample and a different wavelength is re-emitted. The excitation and emission wavelengths are dependent on the molecular structure of the fluorescent material (dye or fluorophore). Since the excitation beam loses some energy the emission beam has lower energy or alternatively larger wavelength. The shift of the wavelength from excitation to emission is called Stokes shift.

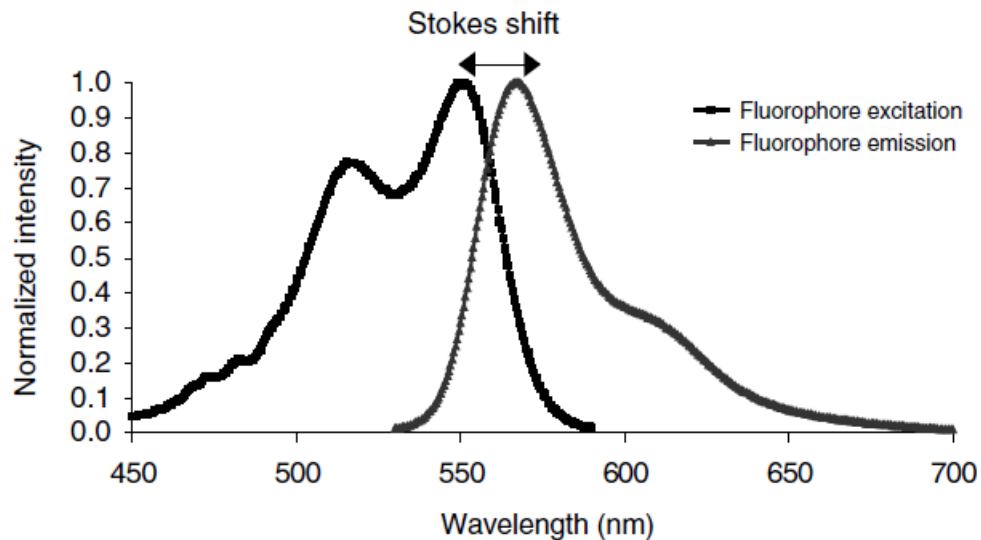


Figure 2.4: Spectrum of the excitation and emission beam [13]. Stokes shift displays how emission peak was shifted toward a larger wavelength.

Fluorescence microscopy is usually done in visible, 380-750 nm [13], spectrum. Although the transmitted fluorescence microscopy is possible, it is usually configured in epi-illumination system. The reason is, easier separation of the excitation and emission beam. If fluorescence microscopy is done in transmitted illumination dark field is preferred, since the distinction between the excitation and emission beam is much easier. As shown in figure 2.5 typically in

fluorescence microscopy a dichroic beam splitter is used. Dichroic mirror reflects the excitation beam and transmits the emission beam. Use of multiple dyes in the sample for simultaneous fluorescence microscopy is possible by utilizing multi-bandpass dichroic mirrors.

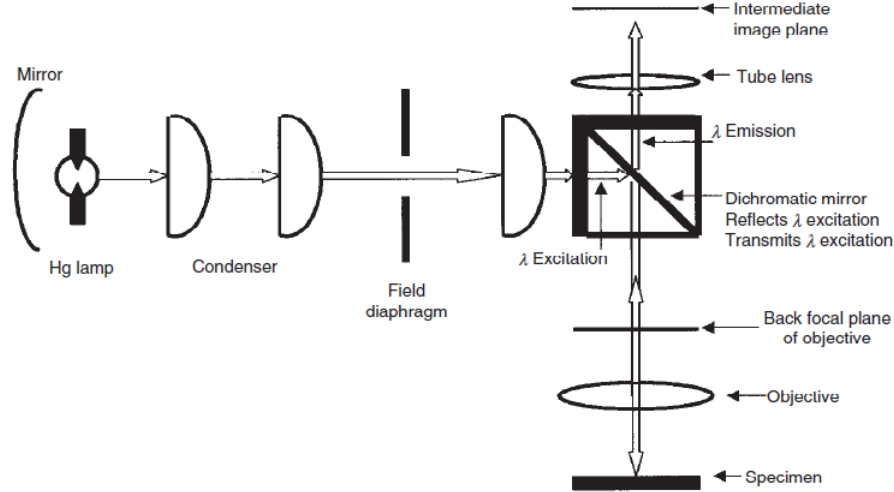


Figure 2.5: Schematics of a fluorescence microscope setup [13]

2.5 Multiphoton microscopy

in the standard one photon confocal microscopy fluorophore absorbs one photon with a higher energy and emits a photon with lower energy. However, if two photons (or multiple photons) can fill the energy gap for excitation of the fluorophore, they can deliver their energy to the fluorophore and excite the molecule. This phenomenon is called two-photon(multiphoton) excitation, and it is depicted in figure 2.6.

Two 800 nm photons, for instance, can transfer their energy to excite molecule with energy band gap of approximately 400 nm. In multiphoton excitation, unlike in the single photon excitation the emission photon has higher energy (or shorter wavelength) than each absorbed

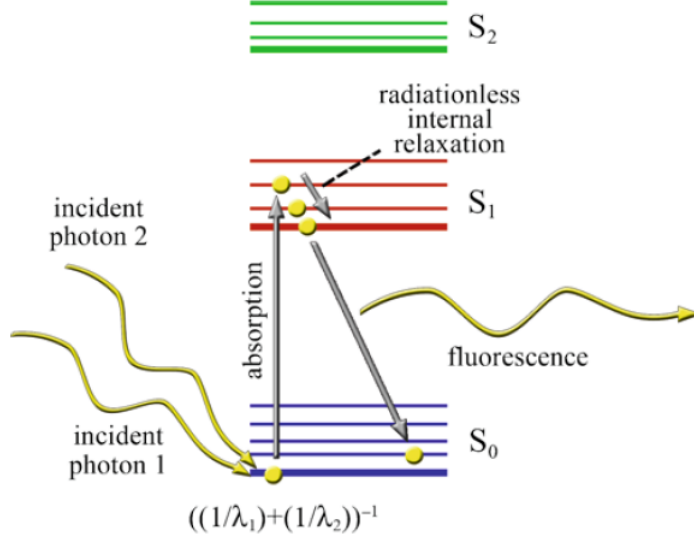


Figure 2.6: Schematic of two-photon excitation [13]. Two photons that strike the fluorophore absorbed and the higher energy photon is emitted.

photon. This huge difference is a substantial advantage, because excitation photon and emission photon can be distinguished much easier. The major disadvantage of two-photon excitation is the probability of the process is lower than single photon excitation. The probability of multiphoton excitation can be represented by the equation 2.1.

$$n_a \propto \frac{p_{avg}^2}{\tau \nu^2} \times \frac{\pi N A^2}{h c \lambda} \quad (2.1)$$

In equation 2.1 n_a represents the probability of multi-photon excitation, NA is numerical aperture of the objective lens, h is the Planck constant, p_{avg} is the average power of each pulse, c is the speed of light, λ is the wavelength of the excitation light, τ is the energy of each pulse and ν is repetition frequency. This expression suggests that for increasing the probability of the multiphoton event a higher power laser source with very short pulses should be used.

The probability of multiphoton excitation far from the focal plane of the objective lens is very low. The reason is, at the focal plane of the objective a large number of the photons are present so the multiphoton absorption effect just occurs in the focal point. Hence, unlike in

the single photon excitation there is no need for a pinhole conjugate to the focal plane. For excitation of atypical flourophore near IR light can be used that has lower Rayleigh scattering cross-section so it penetrates deeper in the specimen. The result is higher signal to noise ratio than in single photon excitation.

2.6 Light Sources in Confocal Microscopy

Since lasers are monochromatic and highly coherent they are commonly used as light sources in scanning confocal microscopy. High energy density of the laser makes detection of the either reflected or fluorescence light more convenient. Normally, a TEM_{00} single transverse mode laser is desired for point scanning confocal microscope. In contrast, wide sources are much applicable for disk spinning microscopy.

Shorter wavelength, like near UV sources, are fruitful for single photon fluorescence microscopy. As discussed previously, equation 2.1 displays that for increasing the probability of multiphoton event fast broad band short pulse laser are substantial.

2.7 Resolution In Confocal Microscopy

As it has been discussed before, resolution in light microscopy depends on the wavelength of the light and numerical aperture of the objective lens. In confocal microscopy lateral resolution is improved by employing a pinhole that excludes the background out of focus light. In order to achieve such resolution improvement, the diameter of the pinhole should be equal to the Full Width at Half Maximum (FWHM) of the Air disk intensity profile. Therefore, optimal pinhole size is slightly smaller than the Air disk diameter. Optimal pinhole size can be calculated by

the following expression, in which NA is the numerical aperture of the objective lens and M is the magnification of the objective [5]:

$$d_{pinhole} = \frac{0.5\lambda M}{NA} \quad (2.2)$$

Lateral resolution of confocal microscope can be calculated from the following formula:

$$r_{lateral} = \frac{0.44\lambda}{NA} \quad (2.3)$$

As Shown in equation 2.3 lateral resolution of the confocal microscope is a little better than conventional wide field microscope. However equation 2.3 is not valid for pinhole size larger than Airy disk. Rayleigh rule states that two close luminous points can be resolved if the dip between them is the 0.74 of the maximum peak.

The axial resolution in confocal microscopy can be represented by the FWHM of the Point Spread Function (PSF) that is calculated by the following expression:

$$r_{axial} = \frac{1.41n\lambda}{NA^2} \quad (2.4)$$

In equation 2.4 n is the refractive index of the medium between objective and sample, λ is wavelength and NA is the numerical aperture of the objective lens.

2.8 Detectors For Confocal Microscopy

The sensitivity of a detector is very significant in microscopy. The detector should have a lower noise, therefore, its signal to noise ratio would be larger which leads to higher contrast images. Since, the sensitivity of the Photomultiplier Tube (PMT) and its Signal to noise ratio is very high it is widely used in confocal microscopy. A PMT consists of a photocathode and

additional curved electrode called dynodes. Photon after hitting the photocathode produces photoelectrons that are accelerated through the array of dynodes. A single photoelectron with enough energy that can produce secondary photoelectron after striking to 10-14 dynodes can produce more than 10^6 photoelectron which is large enough to create the output signal. Consequently, initial input output signal is amplified largely by conversion to electric signal and mapped to a gray scale value for a pixel in the image. This value is proportional to the number of photons absorbed by the photocathode. Figure 2.7 shows the structure of a photomultiplier tube.

The main limitation of the PMTs is their low quantum efficiency (QE), (amount of input

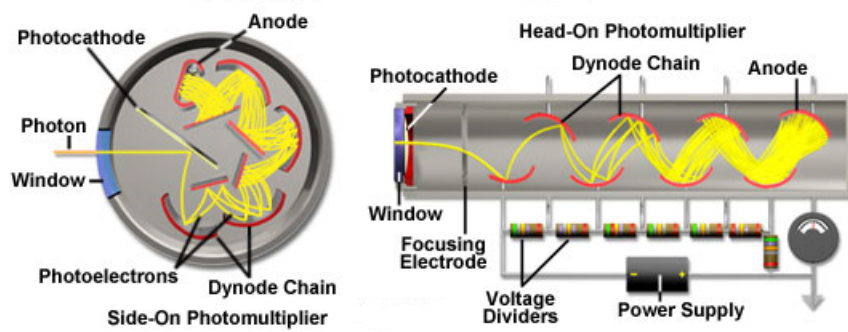


Figure 2.7: Configuration of a typical PMT with array of dynodes. [13]

photons that can generate output signal). Regardless of which location in the sample photos enters the PMT, it maps all of them into a single gray scale value. However it is not a big deal in point scanning microscopy, since each pixel represents a single point in LSCM. Spinning disk confocal microscopes usually apply a cooled CCD camera as a detector.

2.9 Limitation of Laser Scanning Confocal Microscopy

Until now I have mentioned numerous advantages of the Laser Scanning Confocal Microscopy, but it has its own drawbacks. One disadvantage in laser scanning confocal microscopy is high

intensity light illuminating the specimen that can penetrate the plane above and below the focal plane. This process results in damage or photo bleaching of biological samples. The other drawback is low rate of image acquisition in LSCM. This issue arises from the speed limit of the galvanometer mirrors and therefore scanning speed.

Confocal microscope is an elaborate system with some technical consideration for operation. Thus, working with LSCM demands skilled operator or trained users. This makes the maintenance and operation of the LSCM challenging. The user should consider some special parameters, using proper wavelengths, filters, aligning the microscope, etc. Incorrect operating values leads to incorrect data acquisition. The most important drawback of the LSCM system which makes them unfavorable for many researchers or for educational purposes is its price.

CHAPTER 3

Opto-Mechanical development of a Laser Scanning Confocal Microscope (LSCM)

3.1 Optical Setup

In this chapter I am going to describe the LSCM system we developed. Our LSCM components are laser diode as the source, PMT as a detector, galvanometer mirrors for beam steering, Sacn lens, Microscope, Objective lens, and a CMOS camera for real time imaging. I will describe all of them one by one, then I will explain how the LSCM setup work.

3.1.1 Laser Source

Our laser source was a single transverse mode laser diode . This laser's profile was uniform and stable that made it suitable a source for scanning. Please note that we used 532 nm wavelength which is suitable for various samples.

3.1.2 PMT

In the previous chapter I explained how a photomultiplier tube works. Now I am describing the PMT that was used in our setup. A Photomultiplier Tube from Thorlabs (part name: PMM02) was used. It could detect the optical signals from DC to 20 kHz. The output signal at 50 Ω impedance was 0-5 Volts. The PMT could sense a broad range of the wavelengths. The spectral profile of the PMT sensitivity is provided in figure 3.1.

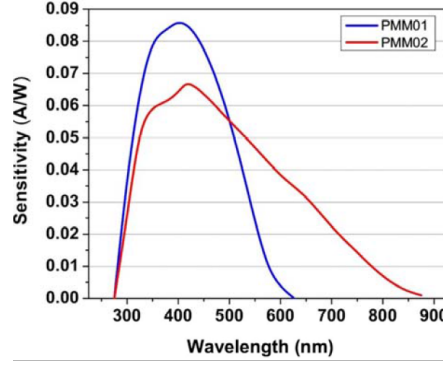


Figure 3.1: Spectral response of the PMT (used in our experimental setup, indicated with the red line) [14].

It was very easy to mount this part to the breadboard and its circular aperture of 1 inch diameter was 1 inch that made it easy to mount any pinhole or filter with diameter of 1 inch. The holes in the front part of the PMT housing made it convenient to use a cage system. I used a cage system and mounted a $f=50$ mm Plano-convex lens in the cage and focused the beam into the center of the pinhole of the PMT. A $75\ \mu\text{m}$ pinhole was mounted on the PMT's aperture (figure 3.2).

3.1.3 Galvanometer Mirror

Galvanometer motors are a limited rotation motors that are used for beam steering. A position detector controls the position of the mirror in a closed loop [1]. We have used a model 6210H optical scanner from Cambridge Technology. One galvanometer scans in X axis and the other one scans in Y axis. The total range of the mechanical scanning for each mirror is 40 degrees and the small angle step response is $100\ \mu\text{s}$. Mirrors dimensions are $22.3\text{mm} \times 9.5\text{ mm}$ [37]. The scanning mirrors are controlled with a driver inside the data acquisition unit which is going to be discussed in Control and Data Acquisition Unit section.

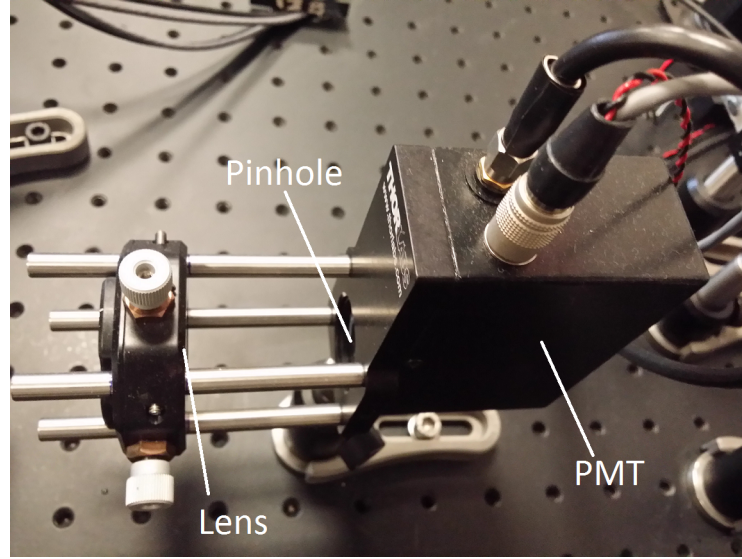


Figure 3.2: Image Of the PMT with pinhole, cage system and lens.

3.1.4 Scan Lens

For having a confocal laser scanning system besides of the galvanometer scanning mirrors a scan lens should be employed. The scan lens should satisfy $F-\theta$ and telecentric conditions. [38]

$f - \theta$ Condition

$f-\theta$ scanning lenses are used in labeling, engraving, cutting and Laser scanning systems. A spherical lens can only form the focus of a collimated beam propagating at different angles relative to the optical axis on a curved plane due to an optical aberration called field curvature. This issue can be corrected by employing a flat plane lens. In an ideal distortion free flat-field scanning lens (see Figure 3.4 B), however, the image height on the image plane will be equal to $f \cdot \tan \theta$ in which f is the focal length of the lens and θ is the beam deflection angle. Hence, the spot on the sample would not have a uniform velocity, and image portions would not be uniformly spaced (pincushion distortion) [39]. This can be corrected by applying some complex algorithms in image processing. In order to avoid the need for such corrections in

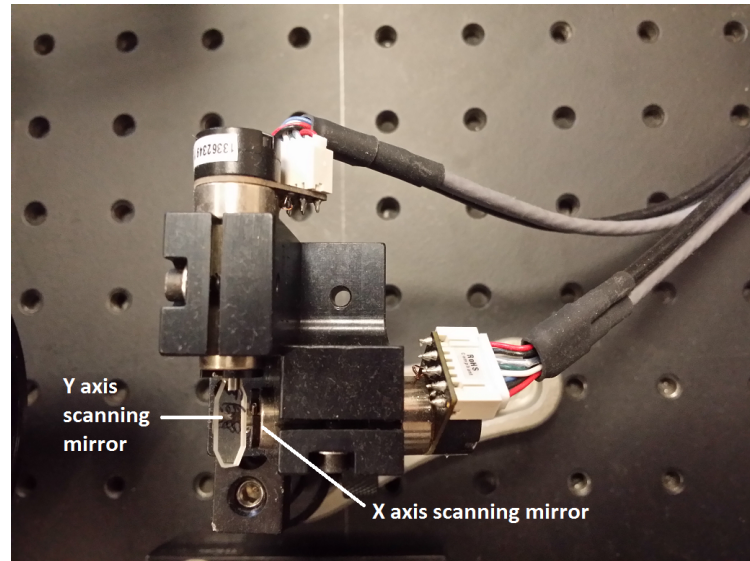


Figure 3.3: Galvanometer Scanning Mirrors :The sample is scanned in X and Y axis by employing two scanning mirrors.

the scanning pattern design and image processing, manufacturers build scanning lenses with a built-in barrel distortion in which the image height that is produced by the scan lens is equal to $f\theta$. By doing so the positioning algorithms are simplified.

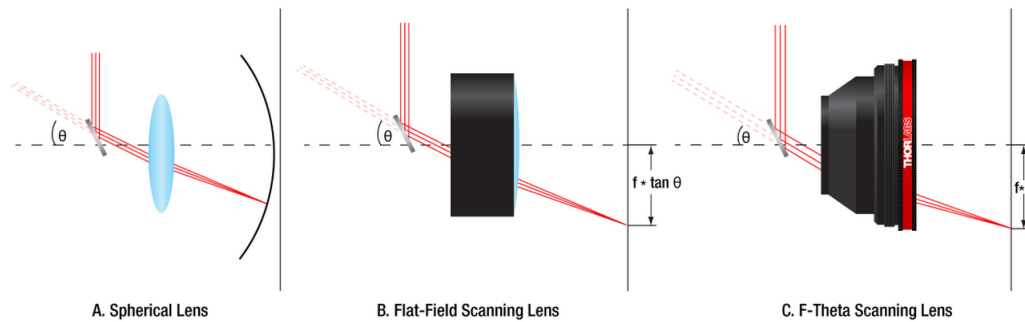


Figure 3.4: Image plane of a Spherical lens (a), a flat-field scanning lens (b) and a f-theta scanning lens [15].

Telecentric Condition

In some applications, like laser scanning confocal microscope, the reflected beam from the

galvanometer scanning mirrors after passing through the scan lens system is used to form the image at a plane that is confocal to object plane (see figure 3.5). This condition requires a telecentric lens in which the focused beam is always perpendicular to the sample surface. This also substantial in some applications such as drilling holes(since the holes should be perpendicular to the surface).

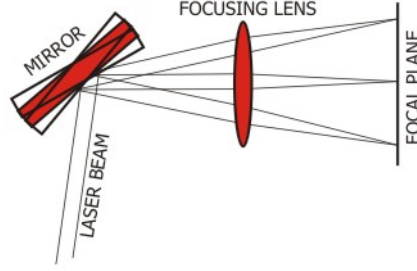


Figure 3.5: Telecentric condition in a scan lens [16].

Thorlabs CLS-SL Scan lens

In construction of the LSCM setup we have employed a Thorlabs F-Theta telecentric scan lens(part name CLS-SL). This lens was designed for point scanning confocal microscopy in visible wavelength range. It can be paired with a tube lens and an infinity corrected objective to form a scanning confocal system. The specifications of the scan lens are provided in table 3.1.

If f_1 and f_2 are the focal lengths of the scan lens and tube lens respectively and d_2 is the distance between the tube lens and objective, in an ideal 4-f system the minimum scanning distance, d_1 (the distance from the scan lens body to the galvanometer mirrors) is 52 mm, the distance between the tube lens and the scan lens is $f_1 + f_2$ and $d_2 = f_2$. However, scanning position can be a little different depending on d_2 . For instance, if d_2 is larger than f_2 then scanning position is closer than 58 mm and vice versa. Therefore, d_1 and d_2 can be slightly

Item	CLS-SL
Wavelength Range	400 - 750 nm
Effective Focal Length	70.0 mm
Lens Working Distance	54 mm
Entrance Pupil Diameter	4 mm (Max)
f/#	17.5
Scanning Position	58 ±6 mm from Mounting Plate
Diffraction-Limited Field of View	16 mm × 16 mm @ 400 - 750 nm (FN 23)
F-Theta Distortion	< 0.05%

Table 3.1: Specification of CLS-SL Scan Lens(FN means field number) [15].

different by δd_1 and δd_2 values and the relation is:

$$\delta d_1 = \delta d_2 \times \left(\frac{f_1}{f_2}\right)^2 \quad (3.1)$$

This condition is displayed in figure 3.6 that shows the optimal values for the scanning configuration. Please note that, this is an afocal system in which an intermediate image is formed between the scan lens and tube lens.

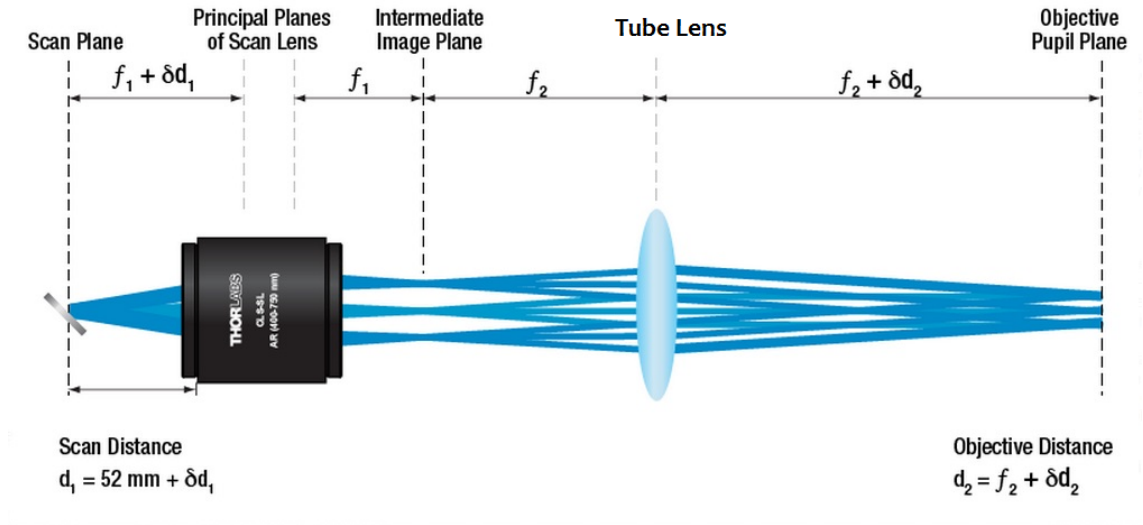


Figure 3.6: Optimal distances for scanning configuration for CLS-SL Scan Lens [15].

3.1.5 Objective Lens

The most important part in a LSCM system is objective. As it was discussed previously, by utilizing a high NA objective with high magnification the resolution and magnification of the system are increased respectively. We have employed a long working distance Nikon Objective (part name: MRP05422). The working distance is 2.1 mm, Numerical aperture is 0.55 and its magnification is 40X. This objective also has a gauge for adjusting the thickness of the cover slip. The objective specifications are depicted in figure 3.7.

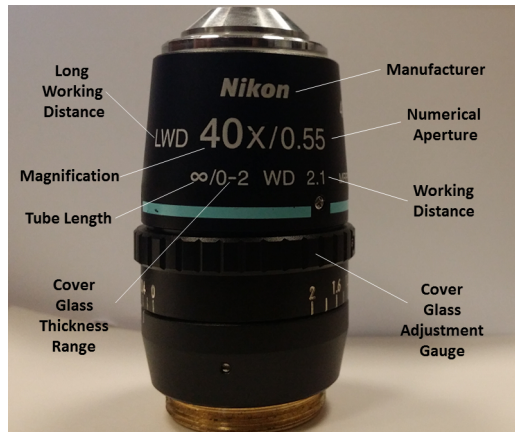


Figure 3.7: Nikon MRP05422 objective specifications.

3.1.6 Microscope Body

We have used an inverted Nikon Ti/U microscope that has four ports including two side ports, one at the back and one for binocular. It was designed for infinity corrected objectives and employs a $f=200$ mm tube lens (see Figure 3.6) to form images at 25 mm distance from the

side ports of the microscope. The magnification is 1.5X and by turning a knob different ports of the microscope can be selected. Filters and dichroic mirrors for various applications can be used. It has two coarse and fine knobs for changing the focus, fine knob can change the distance 100 μm per rotation and the minimum fine reading is 1 μm .

3.1.7 CMOS Camera

For real time imaging we have employed a Thorlabs highly sensitive (Quantum efficiency for $\lambda = 532 \text{ nm}$ is about 60%) monochromatic Complementary Metal Oxide Semiconductor (CMOS) sensor camera (Part name:DCC1240M). Since this is a C-mounted camera, C-mounted camera lenses and filters can be easily mounted on the camera. It is powered by a USB 2 port provided with a computer software. Some aspects of this camera are provided in table 3.2:

Item	DCC1240M Camera
Sensor Type	CMOS
Resolution	1280 \times 1024 Pixels
Optical Sensor Class	1/ 1.8"
Exact Sensitive Area	6.78 mm \times 5.43 mm
Pixel Size	5.3 μ , Square
Frame Rate	25.8 fps
Lens Mounting Thread	C-Mount
Interface	USB 2.0

Table 3.2: Specification of DCC1240M Camera [21].

3.1.8 Filters and Dichroic Mirrors

Applying appropriate filters plays a key role in imaging with a microscope. This is extremely important especially in fluorescence microscopy when a non-monochromatic light source is used for excitation or to ensure that the emission light from the fluorophore is detected and the excitation light is rejected. Filters include long pass (high pass) filters, short pass (low

pass) filters, band pass filters and dichoric beam splitters (mirrors) [13].

In laser applications, photography or imaging usually Neutral Density (ND) filters are applied to reduce the intensity of the light entering the optical system. ND filters have a broad spectral range and they are classified into absorbing and reflecting categories. They are defined by their Optical Density (OD) values. OD of a ND filter and its transmission percent (T) can be calculated from the following formulas:

$$OD = -\log\left(\frac{T}{100}\right) \quad (3.2)$$

$$T = 10^{-OD} \times 100 \quad (3.3)$$

Long pass filters transmit all wavelengths larger than a certain wavelength, called cutoff wavelength, and block the beams with wavelengths lower than cutoff wavelength. On the other hand, short pass filters block the light wavelengths larger than cutoff wavelength and transmit the shorter wavelengths. A band pass filter transmits a certain spectrum of light and blocks the remaining spectrum. Dichoric mirrors are special beam splitters that reflect a certain spectrum and transmit the remaining light. Dichroic mirrors are designed to function at 45 degrees angle with respect to the incident light. the major role of dichroic mirrors in fluorescence microscopy is separating excitation and emission beams.

3.2 Optical Alignment

For doing the optical alignment the first step is aligning the height of the laser beam. Please note that the microscope right port height was 90 mm above the optical table surface, however, there were a galvanometer scanning mirrors in the setup which increased the height of the beam. The distance between the galvanometer mirrors was 6 mm, so I set the initial laser height to 84 mm above the optical table surface. Then, the laser beam should be aligned to ensure that it was completely on the optical axis. In order to align the laser beam, I used two

mirrors with angles 45 degrees to the optical axis, put a diaphragm very close to the second mirror (with respect to the laser light source) and adjusted the first mirror to make certain that the light passed through the middle of the diaphragm. Afterwards, I located the diaphragm farther than the second mirror and this time adjusted the second mirror to ensure that the beam passed through the middle of the diaphragm as much as possible. By returning the diaphragm again close to the second mirror and repeating the previous procedure, I verified that the laser beam was on the optical axis. The next step was adjusting the height of the galvanometer by setting the mirror to their zero degree position and trying to direct the beam to the aperture of the microscope. I put another 2 inch diaphragm in front of the microscope aperture for ensuring that the beam exactly passed through the center of the aperture. This was the toughest part of the alignment that needed great patience and effort.

After ensuring that the microscope port is the right port I checked if the beam goes through the objective mounting socket .Then I used two lenses as beam expander and adjusted their height(I applied two lenses to expand the laser beam with $f_1 = 50mm$ and $f_2 = 100mm$ focal lengths for the first and the second lens respectively). This configuration represented a 2X magnification telescope and the separation between the lenses, was equal to $f_1 + f_2$. Later, I added the scan lens and determined the scanning position which is about 55 mm and the distance between the scan lens and microscope image plane (in fact microscope's images plane was the focal plane of the tube lens) was 52 mm. Consequently, I added the objective to the system.I placed a beam splitter between the microscope and scan lens, then using a Thorlabs doublet (part name: MAP1050100-A) in front of the camera ,I obtained the real time images. Then , a dichroic mirror was added to obtain images with the PMT. The final step was aligning the height of the PMT,constructing a cage system with a $f = 50mm$ Plano-convex lens and placing a $75\ \mu m$ pinhole in the aperture of the PMT.

Precise optical alignment of the PMT was significant for obtaining clear images. I used a signal generator to applying proper voltage to one of the scanning mirrors. Then by applying a

appropriate control voltage to the PMT, adjusting the location of the PMT and then position of the lens in front of the PMT, I attempted to see the powerful noise-free signals on the oscilloscope. In addition, I applied two ND filters after the laser, a ND filter with OD=3 and variable ND filter for reducing the intensity.

3.3 How LSCM Setup Works:

Figure 3.8 displays the final LSCM setup in which all of the parts are labeled. I explain how the LSCM setup works in the following:

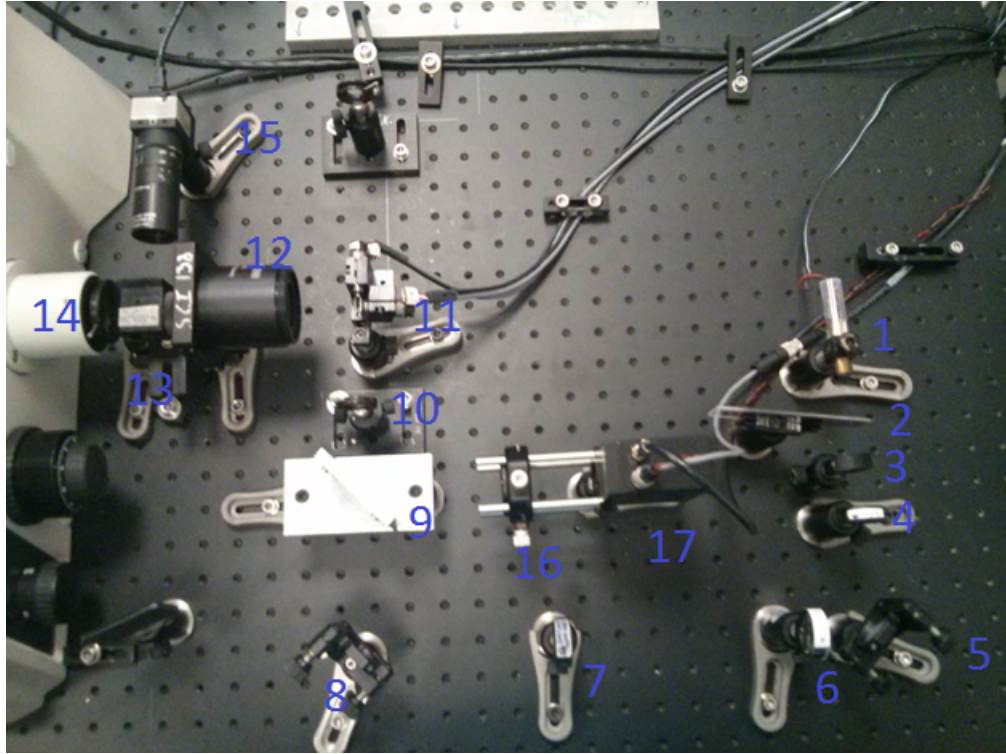


Figure 3.8: 1- Laser source ($\lambda=532$ nm), 2- Continuously variable, metallic neutral density (ND) filter for altering the intensity, 3- ND filter, 4-Plano-convex lens $f=200$ mm, 5-Mirror, 6- Plano-convex lens $f=50$ mm, 7- Plano-convex lens $f=100$ mm, 8- Mirror, 9- Dichroic Mirror 10- Diaphragm, 11- Galvanometer (Scanning Mirror), 12- Scan Lens $F=70$ mm, 13- Beam Splitter, 14- A tube lens and microscope objective (40X, 2.1mm working distance, $NA=0.55$), 15-Camera for obtaining real time images, 16- Convex lens $F=50$ mm, 17- Photo Multiplier Tube (PMT) .

1. Laser source: It is a green $\lambda = 532$ nm single mode laser diode. The power is 5mw and

the profile quality is decent.

2. A ND filter for reducing the intensity of the laser beam.
3. A variable ND filter to control and reduce the intensity of the beam.
4. The laser beam passes through a plano-convex $f=200\text{mm}$ lens that converges the light.
5. Beam strikes a mirror and it is reflected to the next lens.
6. A plano-convex $f=50\text{ mm}$ lens.
7. Beam travels and passes through another plano-convex $f=100\text{ mm}$ lens. Together with lens 6 this configuration is a 2X beam expander.
8. Beam is reflected by another mirror.
9. beam passes through dichroic beam splitter and reaches galvo -scanner.
10. A diaphragm for regulating the amount of light that passes through the Galvanometer scanning mirrors.
11. Galvanometer scanning mirrors for beam steering: The fast motion mirror provides scanning in X axis and the slow one provides scanning in Y axis.

12. A scan lens: By using a scan lens with microscope objective, LSCM systems can provide an image area more than 100 times that of a standard microscope. Our scan lense has back focal length of 70mm.
13. Second beam splitter for obtaining real time images with camera
.
14. There is a tube lens inside the microscope. The focal length of tube lens is 200mm. By putting the sample in the exact focal length of the objective(it is an infinity corrected Nikon 40X objective with working distance of 2.1 mm and NA=0.55) rays after scattering from the sample go through the objective lens and parallel rays comes from the exit pupil of the objective.
15. Some portion of paraxial rays passing from the tube lens and reflected by the beam splitter reaches to the USB camera which was plugged into a computer.
16. Another portion of the beam goes through the beam splitter, was reflected from galvanometer scanning mirrors, reflected by the first beam splitter and reached the PMT lens. This lens focuses the rays to detect them by PMT.
17. Finally the beam reaches the PMT. It is an extremely sensitive detector of light.

3.4 3D CAD Drawings of The LSCM Setup

I started drawing some parts with solidworks. First I worked on drawing some simple parts then designed more complex parts. Then I applied material properties to the parts. Figure 3.9 depicts some microscope parts and the breadboard that I designed.

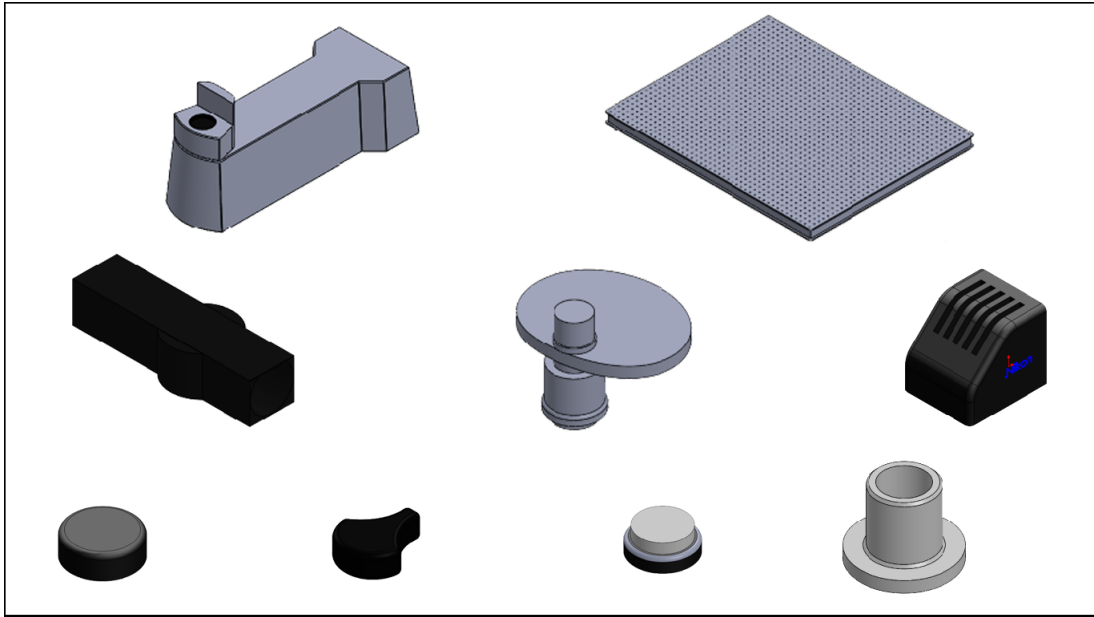


Figure 3.9: Schematics of some parts designed in solidworks.

I also downloaded some 3D drawings of optical components provided by Thorlabs website. The next step was assembling these parts to construct the setup. The most challenging part was the microscope body part that consisted of more than 50 parts. The schematic of 3D drawings of microscope and the optical setup is illustrated in the following figures.

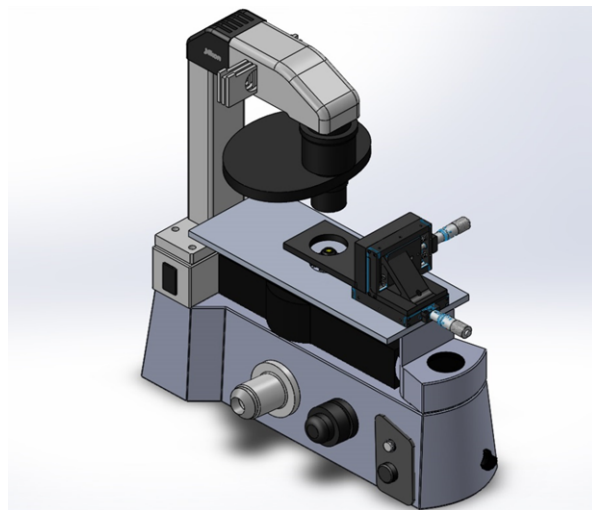


Figure 3.10: Schematics of 3D design of the microscope

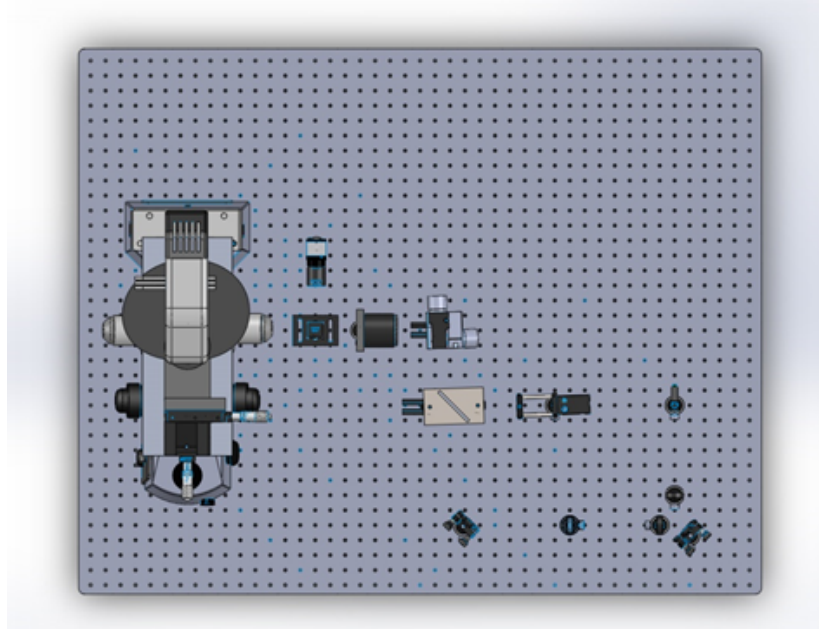


Figure 3.11: Top view of 3D drawing of the optical setup.

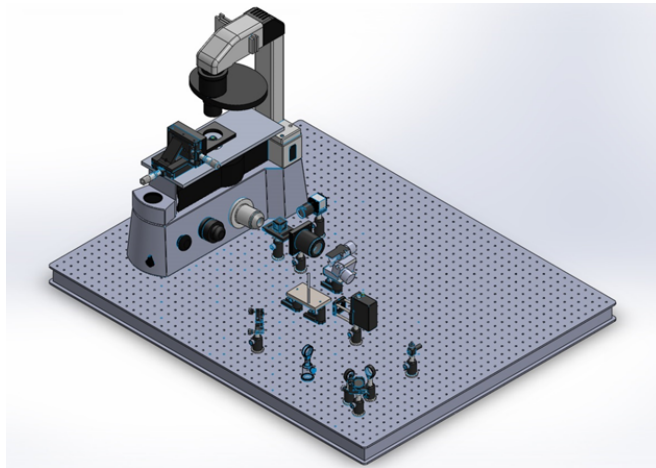


Figure 3.12: Side view of 3D drawing of the optical setup.

3.5 Control and Data Acquisition Unit

This unit controls the LSCM system by providing power source of the system and controlling the mirrors and obtains data from the PMT. The flowchart of the LSCM setup is provided in

figure 3.13.

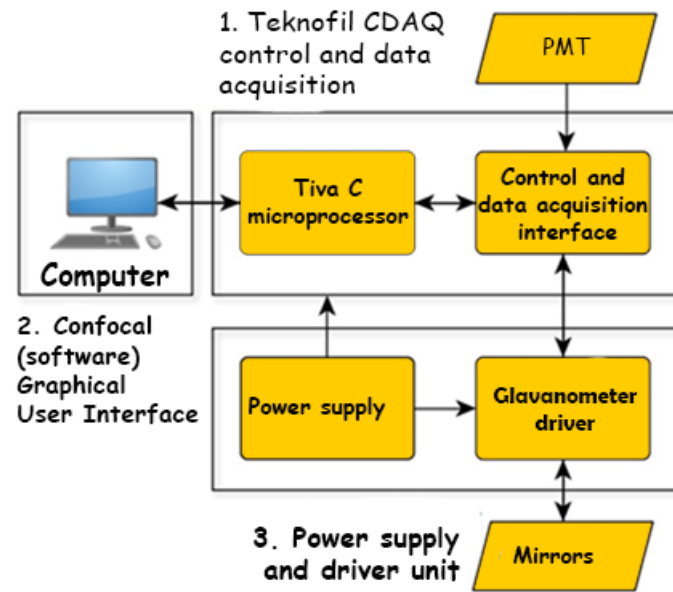


Figure 3.13: Flowchart of the LSCM system

The control unit includes the power supply, galvanometer driver and the data acquisition part, and a Texas Instruments Tiva launch pad. Therefore, there is no need for external power supplies and electronic chips. The following figure shows data acquisition and control boxes.



Figure 3.14: Control and data acquisition unit.

3.6 Confocal Software

For obtaining images there should be a graphic user interface. By the help of a program developed in Python, imaging with our LSCM microscope is accomplished. This was an advantage, since there was no need for extra programs, like Lab view, for imaging and data acquisition. In addition users can alter the source code and develop their own programs. The system and screen shots from the confocal software are provided in figures 3.13 and 3.15 respectively.

After running the program, for initiating the scanning go to menu select new session and enter the session name. Then by selecting the session and clicking on the new scan a window like figure 3.16 will pop up. Afterwards, the scan range and step size for X and Y should be entered (See figure 3.16). For instance, If the scan range is entered between 10000 and 20000 and the step size is 50, the numbers of pixels in X can be calculated by the following:

$$\frac{20000 - 10000}{50} = 200 \text{ pixels}$$

Same approach is valid for Y axis. Then, wave form that is going to be applied to galvanometers should be chosen. The last option is DAC speed that controls the scan speed and ranges between 0 to 100%. Finally, by clicking next bottom, scanning will start and at the end an image is created.

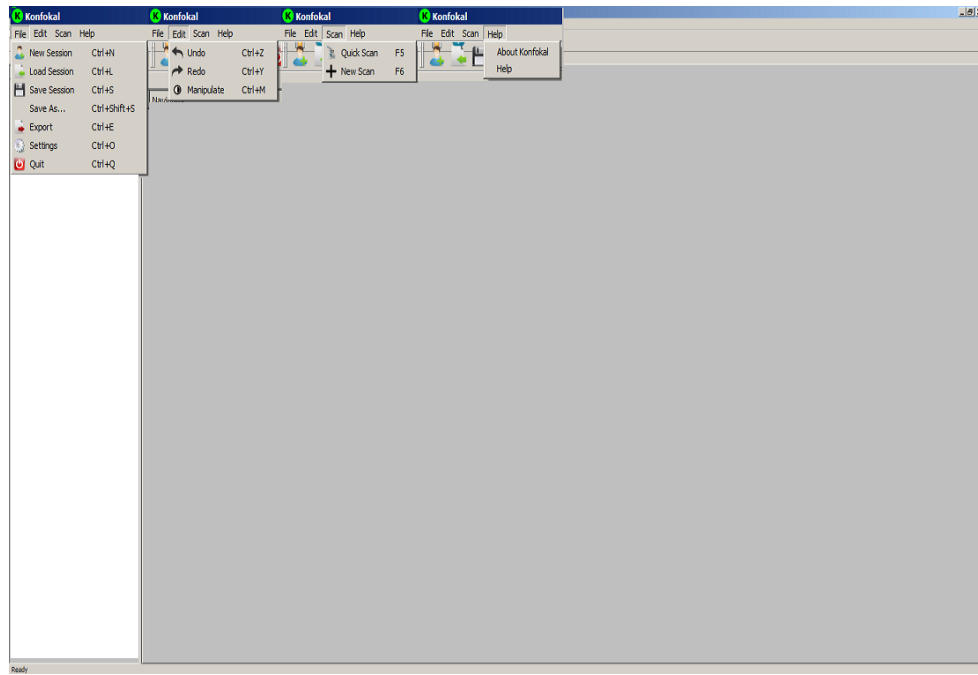


Figure 3.15: Confocal program graphical user interface.

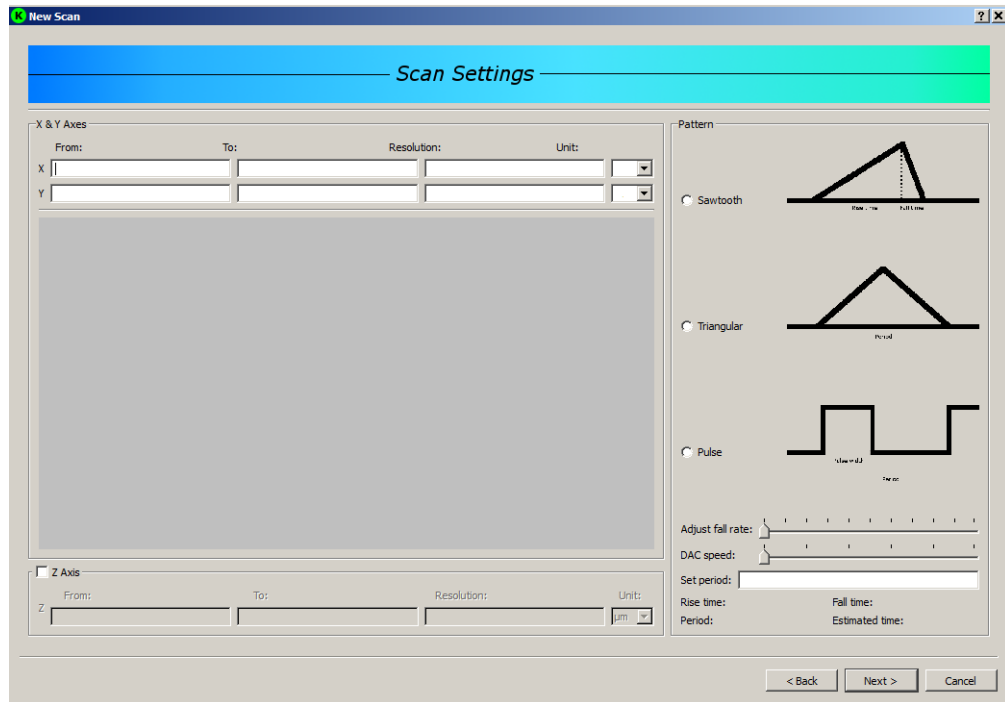


Figure 3.16: Scanning values are entered to the system from this window.

3.7 Simulations With Zemax

Zemax is a program for optical design and simulation. Zemax can analyze and simulate the systems in ray optics and physical optics. Optical systems such as mirrors, lenses, fibers, light sources, aspheric lenses , etc can be modeled and analyzed in Zemax. [7] [40].

In Zemax ray tracing is possible in sequential ray tracing mode (in which rays goes through the optical surfaces one by one until the last surface) or non-sequential ray tracing mode. Many diagrams can be drawn in Zemax for analyzing the optical system such as, spot size diagram, Foot print diagram, ray fans, MTF diagram, 3D and 2D diagram, etc. Zemax has a very good library of commercial lenses which can be easily added to the system. Different coatings for optical components such as mirrors, beam splitters and lenses is also possible.

I worked with Zemax, in standard sequential ray tracing mode. In this mode the beam strikes the surfaces one after another from left to right. To start simulations with Zemax, I had to understand how to model a laser source, how to modify general configuration of the setup such as aperture, changing the stop surface and, how to produce standard analysis diagrams, and to work with field angles [41].

3.7.1 Simulation Procedure

1. I designed the system in the sequential mode so the beam goes through the first surface and then proceeds until the last surface.
2. The system was designed and analyzed in ray optics.
3. The optimization was done to decide the optimal distances.
4. After calculation the optimal angle range for the scanning mirror, I have used one scanning mirror to scan between 3 to -3 degrees.
5. I have made three configurations for 3, 0 and -3 degrees scan angles and showed the results of different analysis for these configurations 3.17.

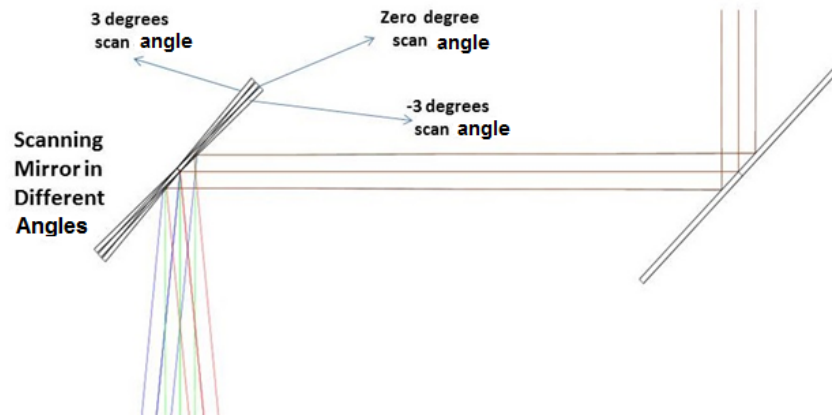


Figure 3.17: Three configurations of the scanning mirror that represents three scanning angles.

6. The stop of the system could be on the Scanning mirror or on the scan lens.
7. The scan lens and tube lens make an afocal system and intermediate image of the sample is formed between them. The ratio between focal lengths impacts the final magnification.

Note: You may find the general design information and details at the appendix.

3.7.2 3D Diagram of The Setup

The 3D shaded figure of the LSCM system is the following. All the parts were labeled in the figure.

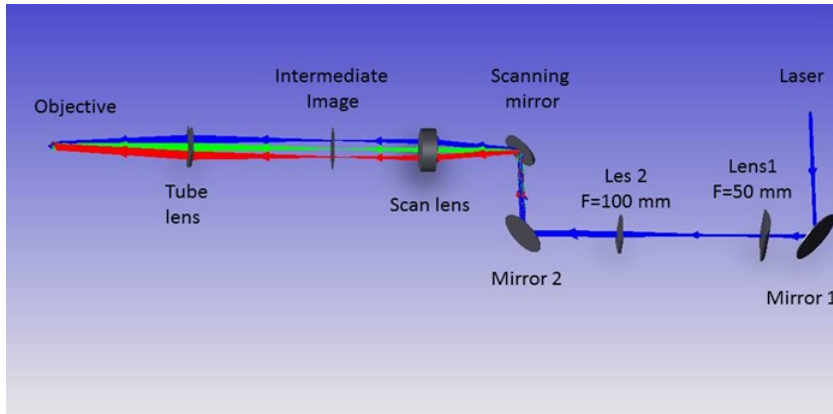


Figure 3.18: 3D diagram of the LSCM system in Zemax

3.7.3 Spot Size Diagram

Spot size diagram traces bundles of rays through the system to the specific surface to show ray distributions (see Figure 3.19). This analysis indicates the pattern of rays as they appear in the image plane. The RMS value can represent the system resolution in the presence of aberrations.

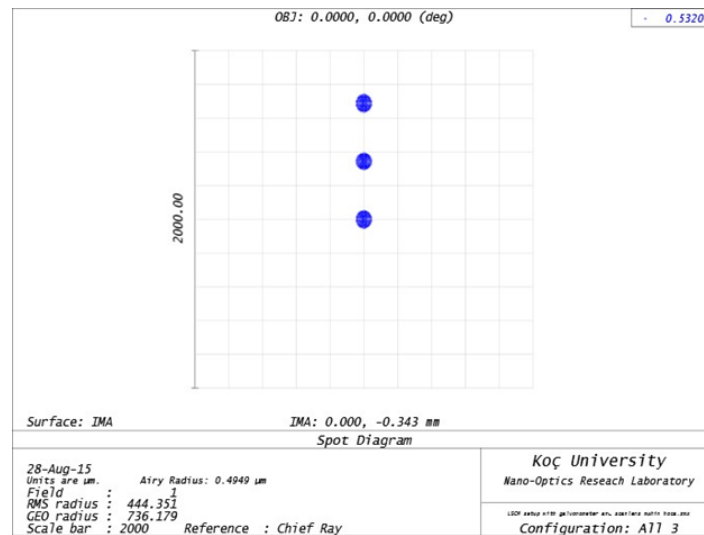


Figure 3.19: The standard spot diagram at image plane for the three scanning configurations, 3, 0 and -3 degrees.

3.7.4 Footprint Diagram

This diagram indicates the footprint of the bundle of light superimposed on the surface. Figure 3.20 indicates the location of the beam in three different 3, 0 and -3 degrees scan angles at image plane. The scan range is 800 μm as it was illustrated in the following figure.

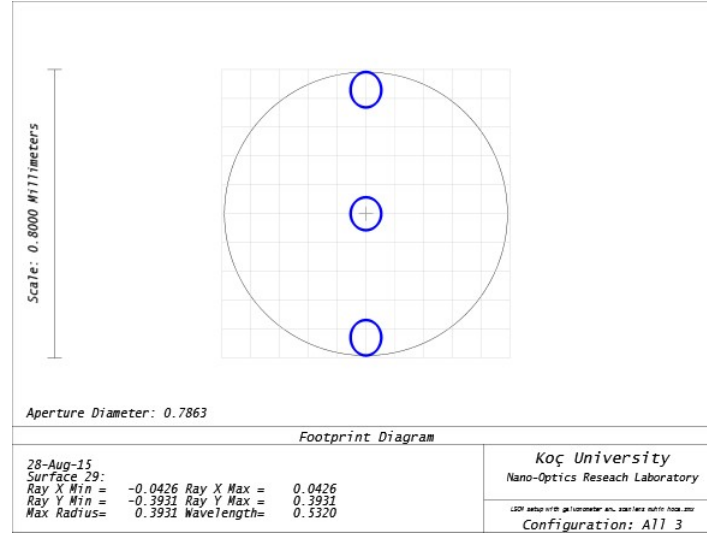


Figure 3.20: The footprint Diagram at image plane for the 3, 0 and -3 degrees scan angles

3.7.5 MTF Diagram

The diffraction modulation transfer function (MTF) diagram calculates the MTF data positions with FFT algorithm for all fields. It is a very important factor in imaging, since it is a way to incorporate resolution and contrast in one Function [42]. The following figures displays the MTF for three different configurations:

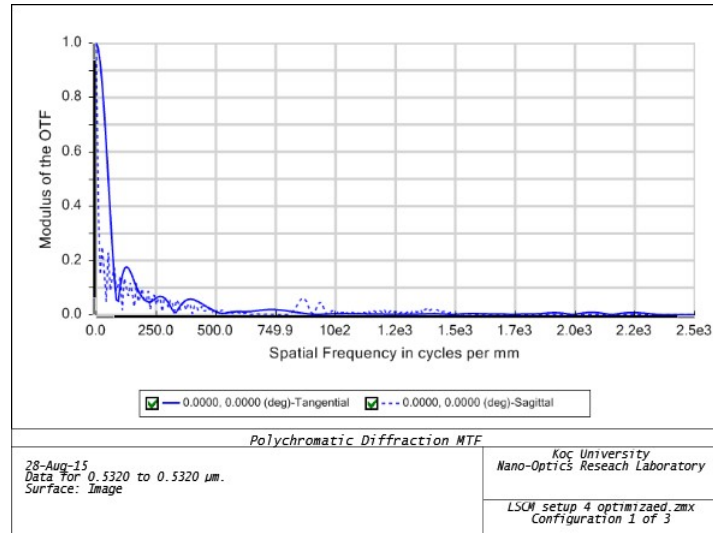


Figure 3.21: FFT MTF diagram for the first and third configurations, 3 and -3 degrees scan angle.

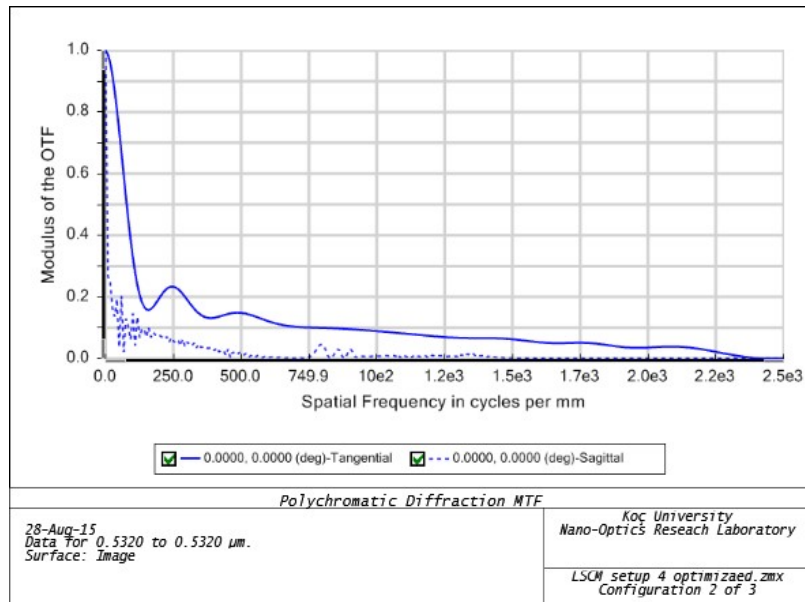


Figure 3.22: FFT MTF diagram for the second configuration, zero degree scan angle.

From these figures the diffraction limit of the system can be calculated by Zemax. If we take zero degree as the reference configuration, the following figure displays the diffraction limit at the tangential plan happens in 2200 spatial frequency. Diffraction limit can be calculated by dividing 1 mm by 2200 which is equal to 454 nm.

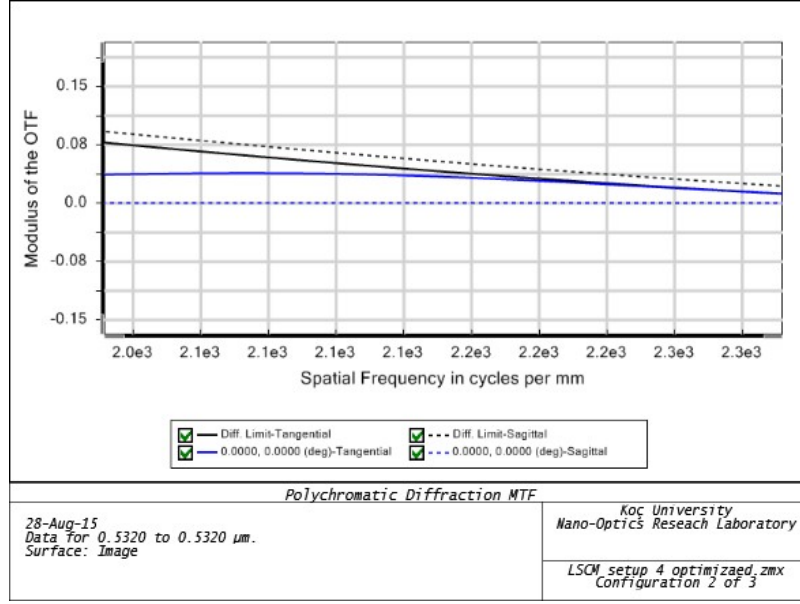


Figure 3.23: Diffraction limit of the system occurs at 2200 spatial frequency.

3.8 Spot Size Analysis of LSCM setup

I have analyzed the spot to calculate the spot size and ensure that if the image of the spot size on our camera was saturated or not. The initial spot was large (about $3 \mu\text{m}$) and was not circular, which arose from the scan lens position and optical misalignment .

I have applied different ND filters to analyze the spot size image on the camera to ensure that it is not saturated. In order to make sure that the image is not saturated I draw the 3D surface plot in Imagej and analyzed image matrix in Matlab (see figure 3.24). After, finding an appropriate ND filter, I changed the focus to have the smallest spot size(see figure 3.25). Afterwards, by changing the focus step by step($5 \mu\text{m}$ for each step) I increased the distance of the objective from the sample. Afterwards, I returned to the initial focus distance (in which the spot size was minimum), however, this time I decreased the objective distance from the sample step by step ($5 \mu\text{m}$ for each step).

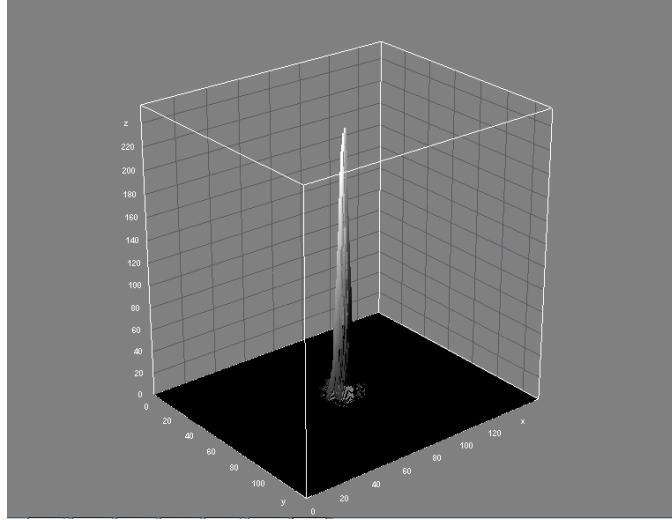


Figure 3.24: 3D surface plot of the minimum spot of the LSCM setup.



Figure 3.25: Minimum spot of the LSCM setup.

I fitted Gaussian function on the images of different focal shifts with (Origin program) to find the spot size at full Wide Half Maximum (FWHM) for each image. Afterwards, I draw the spot size at FWHM versus focal shifts graph(see figure 3.26. In this graph I supposed that the focal shift of the minimum spot size at FWHM is zero and negative values of the focal shifts means the objective is farther than sample from the reference minimum spot size point

Additionally, positive values mean that the objective is closer to the sample than the reference minimum spot size point.

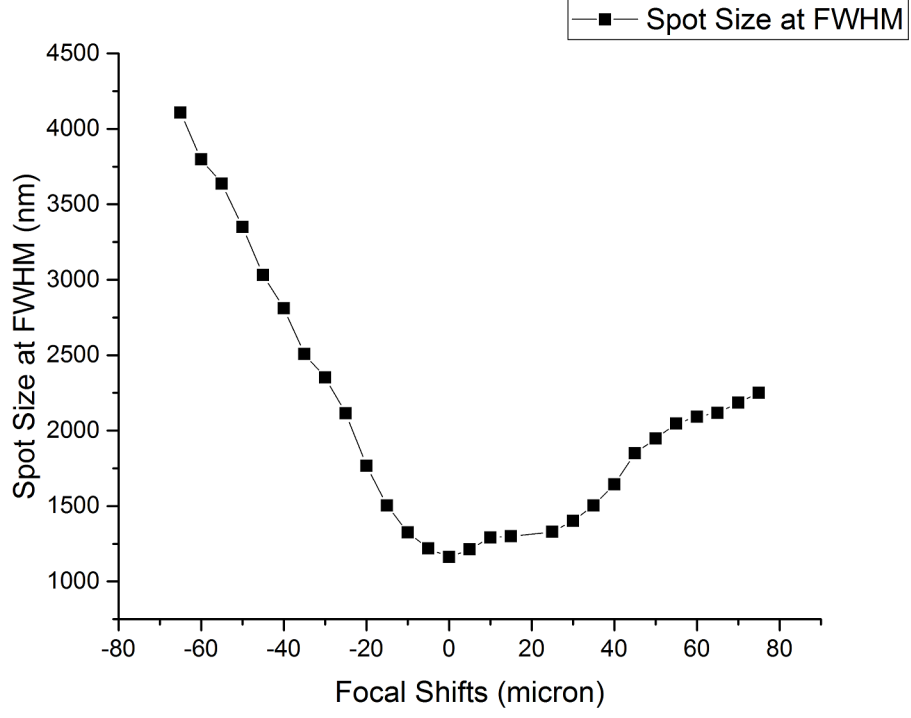


Figure 3.26: Minimum spot of the LSCM setup.

As shown in figure 3.26, if the distance of the objective from the focal plane is decreased to the sample spot size value is increased. On the other hand if the distance of the objective from the focal plane is increased to the specimen spot size is increased, but this time the rate of increasing is much more higher. Figure 3.26 indicates that the minimum spot size at FWHM of the LSCM setup is $1.162\mu m$.

$$Minimum Spot Size_{FWHM} = 1.162\mu m \quad (3.4)$$

3.9 Scanning Results of The LSCM Setup

Initial imaging experiments were done with a microscope calibration ruler, in which the distance between the center of two adjacent lines were $10\text{ }\mu\text{m}$. Therefore, we could calibrate our microscope. I first applied saw tooth waves to the galvanometer scanning mirrors, but noticed that the scanning speed is so low(1 frame per 8 minutes for a 100×100 image)and after 10 minutes galvanometers experiences a lot of heat. By applying triangular waves galvanometers mirrors performance was improved and the heat was not an issue anymore. The pixel size of the image could be modified easily by the confocal program. In addition the scan range also can be controlled in X and Y dimensions. Figure 3.27 displays a 100×100 pixels image that was obtained by the confocal program. I have used a 40X NA=0.55 objective.

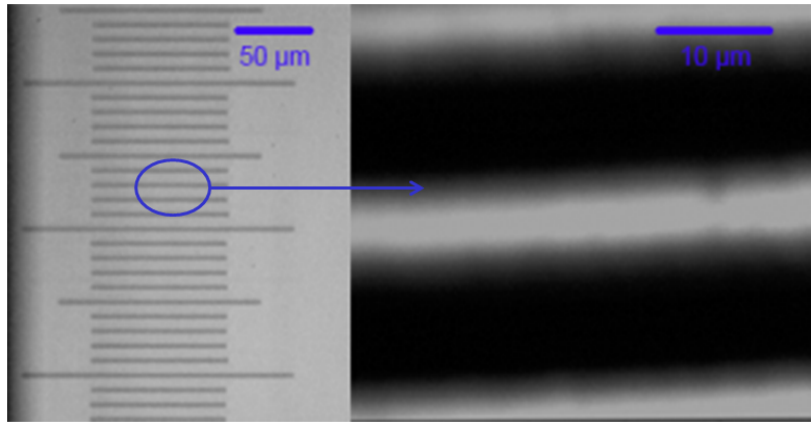


Figure 3.27: sample (left) and the image obtained by the LSCM (right)

CHAPTER 4

Digital Micromirror Device (DMD) Based Microscope

4.1 What is a Digital Micromirror device (DMD)?

Digital Micromirror Device microelectro-mechanical (MEM) (DMD) is a chip developed by Texas Instruments that consists of a tiny mirror arrays. In a DMD chip each mirror represents a pixel and has two operational states defined by the angle between the normal direction of the mirror and the normal direction of the whole chip (+12 and -12 degrees) [17]. These states determine the direction of the reflected light. If a mirror is tilted toward the illumination light it is in ON or positive position. Conversely, if a mirror is tilted away from the light source it is referred to be in off or negative position. Put in other words, DMD is a Spatial Light Modulator (SLM). Figure 4.1 displays on and off states of for DMD mirrors.

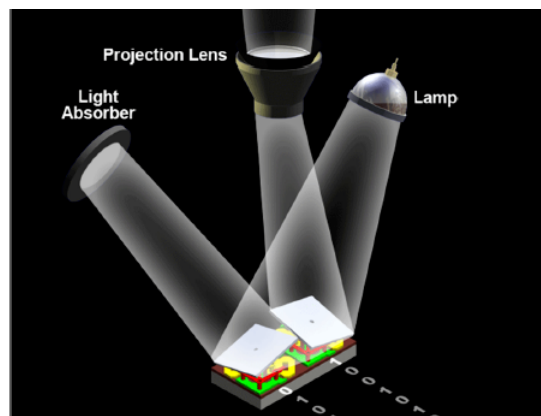


Figure 4.1: Two operational states of the DMD chip. [17].

Generally speaking DMD chips are provided with a light engine and electronic chips for controlling the mirrors; this module is called Digital Light Processing (DLP) module. Various DLP modules employ DMD chips with different resolutions and light engines. DLP 4500, for instance, employs a DMD chip with 912×1140 mirrors and a RGB LED source with 150 lumens output power [43].

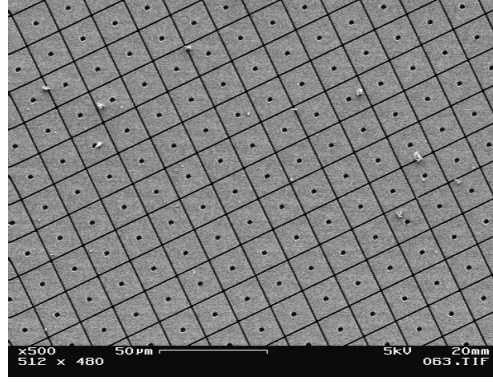


Figure 4.2: Image of the DMD mirrors with SEM microscope [18]

Recently, DMD chips have been widely used in projection , 3D printing, face recognition , mounted displays [44, 45], and even in microscopy [46, 47] [48]. Nowadays, DMD application in microscopy is very popular, since DMD based microscopes have high scanning speed due to parallel scanning [49]. In one novel approach a DMD based super-resolution microscope was successfully developed [50]

4.2 DLP LightCrafter Evaluation Module (EVM)

Since in our project we have employed a DLP LightCrafter EVM, I am going to explain its configuration. DLP LightCrafter EVM consists of three major parts: light engine, Driver board and System board. Driver board includes LED drivers, DMD driver, power management chips and MSP430 micro controller. System board consists of FPGA and external input connectors [19].

The light engine serves optical unit of the DMD. It involves: Three RED, BLUE and Green LEDs with 20 lumens flux intensity (can be increased to 50 lumens but an external fan is required), a WVGA 0.3 inch DMD chip(DLP3000) with 415872 mirrors in a 608×684 array. As shown in figure 4.3 the mirrors are arrayed in a diamond pattern and have dimensions of $7.63 \mu m \times 7.63 \mu m$.

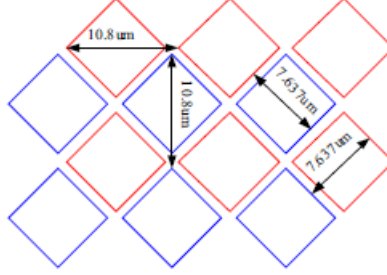


Figure 4.3: Mirror arrays in DLP3000 DMD chip. [19]

To understand how light engine operates its inside structure is discussed below. Figures 4.4 and 4.5 shows the light engine parts from top and bottom view. There is a collimator lens in front of each LED. Two dichroic beam splitters direct the light from LEDs to a micro lens array. This lens array is utilized to make the illumination uniform on the DMD chip. Then, light passes through a condenser lens and converges through a mirror that reflects the beam to the DMD chip. Finally, light deflected by the DMD's tiny mirrors goes through a projection lens and an image is formed.

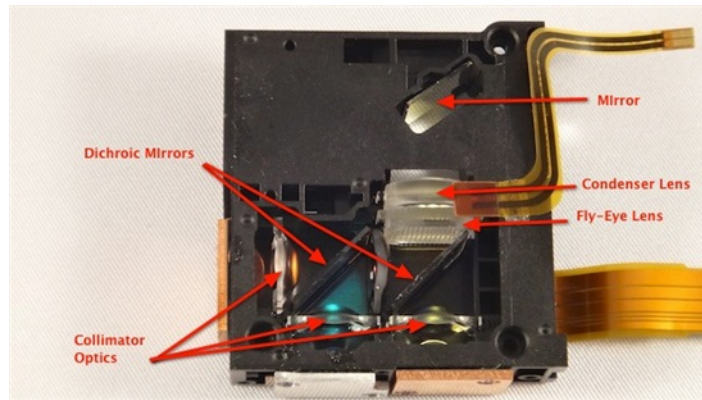


Figure 4.4: Inside of the light engine of the LightCrafter EVM (top view) [20].

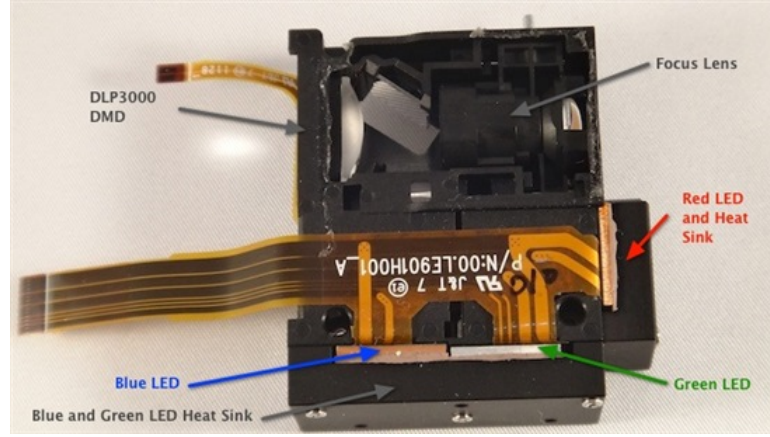


Figure 4.5: Inside of the light engine of the LightCrafter EVM (bottom view) [20].

4.3 Developing a DMD Based Microscope

Nowadays, there is a new trend in microscopy, which utilizes DMD chips mainly in bioimaging. The major advantage of using DMD in microscopy rather than a conventional galvo scanner is faster scan rate without reducing the signal to noise ratio. It is like applying a parallel confocal configuration. In one of references [51] by implementing a 100x objective with $NA=0.9$ and a 800×600 resolution DMD they have reached lateral resolution of 0.4×0.4 micron and axial resolution of 0.8 micron.

In constructing the setup I should make certain that confocal condition which is 3 conjugate focal points (illumination point, sample point and detector point) is achieved. As mentioned previously, state of the mirrors are $+12$ or -12 degrees which represent ON (onto sample) or Off (off of the optical system) state. By changing each mirror successively from off position to on position the entire image will be formed.

For constructing the setup there were two possibilities. The first one was employing DLP LightCrafter EVM light engine for the sampling. The other option was utilizing our own laser source by removing the light engine of the DLP. Considering versatility, we removed the light

engine and used an external laser source. The schematic of the optical setup is shown in Figure 4.6.

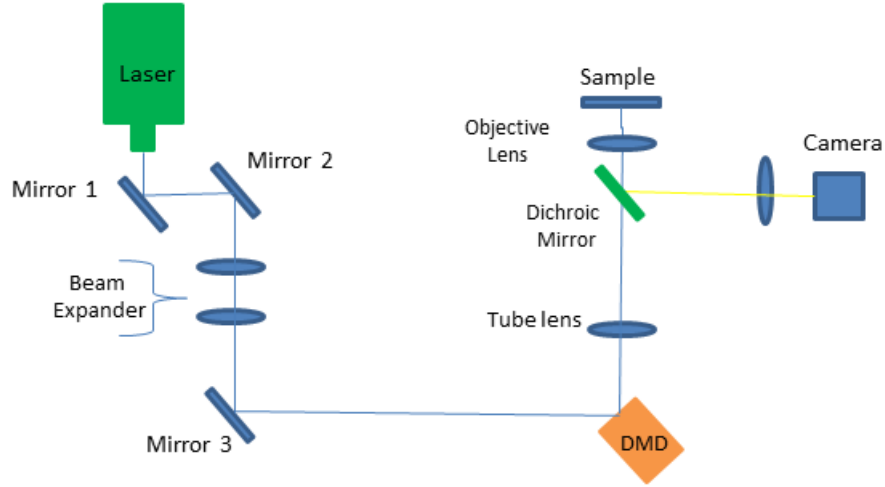


Figure 4.6: Schematics of the DMD based optical setup

4.4 Optical Alignment

Identically to the galvanometer-based confocal setup, I started with adjusting the laser height. I employed two mirrors to direct the laser beam (see Figure 4.6). Next, to ensure that the laser beam is on the optical axis, I put a diaphragm just close to the second mirror and adjusted the first mirror screws to locate the beam in the middle of the diaphragm. Then, I moved the diaphragm farther from the second mirror, but this time adjusted the second mirror to have the beam at the center of the diaphragm. By repeating this process, I made certain that my beam was on the optical axis. I used the third mirror and aligned the beam to strike the DMD surface. I employed a beam expander like in the previous setup, however, a 2X telescope was inefficient since the beam did not cover the whole surface of the DMD chip. Therefore, a 4x beam expander was used to achieve the desired illumination. Then I connected the DLP to the computer, run the graphic user interface and by applying a white pattern, I made all the

mirrors in positive position. Then, I positioned the DLP chip at +24 degrees respect to the optical axis to lead the beam inside the microscope aperture (see figure 4.7 and figure 4.8).

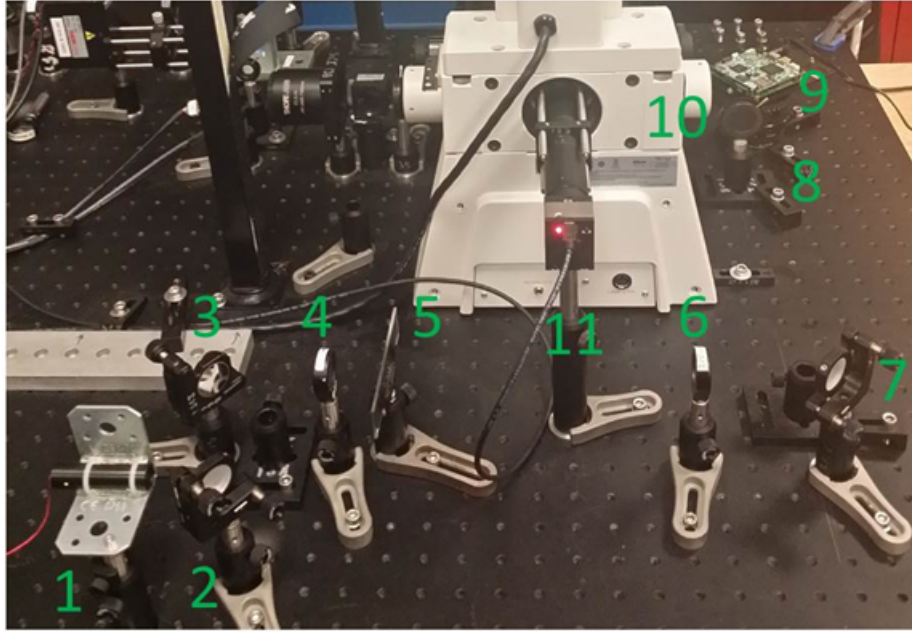


Figure 4.7: DMD based microscope optical setup: 1.Laser, 2.Mirror 3.Mirror 4.Plano-convex lens $f=50$ mm 5.Variable ND filter, 6.Plano-convex lens $f=200$ mm 7.Mirror 8.Diaphragm, 9.DMD 10.Tube lens and objective, 11.Camera.

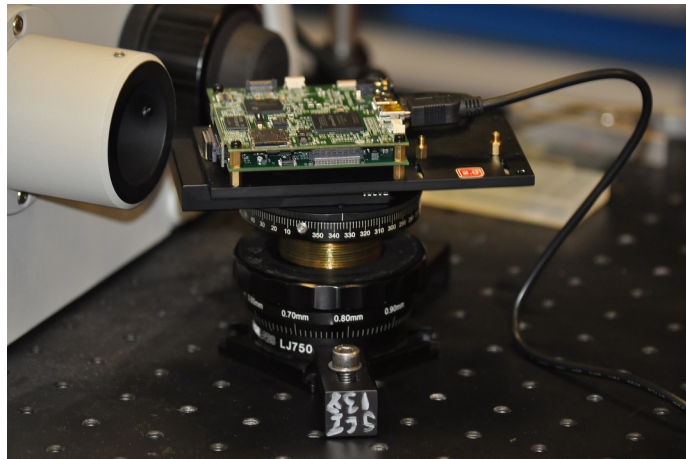


Figure 4.8: DLP chip and its holder.

Please note that the DMD active area was on the image plane of the microscope. Using a

NA=0.55 and 40x objective I checked if the beam went through the objective. Then, I aligned DLP chip precisely to see the image of the DMD at the focal (sample) plane of the objective.

There were some considerations:

1. At first I used a $\lambda = 532$ single mode laser diode with decent power(10 mW). However, there was an issue, with passing time the profile of the laser was changed. Hence, I had to change the laser source and replaced it with a new laser (5 mW single mode laser pointer operating at $\lambda=532$ nm) that had a much more uniform profile. That was important since it significantly affected the illumination of the DMD's active area. Poor profile of illumination beam results in blurry and poor quality images.
2. I added a continuously variable, metallic neutral density filter to easily control the beam intensity on the DMD surface.
3. In the beginning there was an issue with aligning the DMD. It was very hard to make sure that if the DMD was in the desired angle that patterns were projected on the sample. Therefore, a better holder with the possibility of fine adjustment of the DMD angle was used for the DMD and that made the alignment much easier(see figure 4.8).

4.5 How The DMD Based Setup Works?

The DMD based microscope setup is displayed in figure 4.7 in which all the parts are labeled. Here is how the setup works:

1. Laser source: Again 532 nm wavelength green laser source was employed. This laser's profile was uniform and stable which made it suitable as a source for DMD. 532 nm wavelength was used due to its adaptability for various samples.
2. A Plane Mirror: Laser Beam hits surface of a plane mirror and is reflected to the next mirror

3. Second Plane Mirror: Beam hits the surface of this mirror and goes through the first lens of the beam expander (lens labeled 4). This is a z shape configuration for better aligning the laser beam.
4. First lens: Beam goes through the this plano-convex $f=50$ mm lens that is a part of the beam expander.
5. variable ND filter: Beam goes through a variable, metallic neutral density filter and by moving the filter to the left and right I could control the beam intensity.
6. Second Lens: This is a plano-convex $f=200$ mm lens which forms the second lens of the a beam expander to make the beam width large enough to cover the active area of DMD. By using this beam expander, I made the beam diameter four times larger.
7. Mirror: Beam hits the surface of the mirror and it is guided toward the DMD chip.
8. Diaphragm: There is a large diaphragm and the size of the aperture regulates the amount of light that goes through the DMD chip and cancels unwanted glare.
9. DMD: beam hits the surface of the DMD. If the mirrors are in on position they reflect the beam inside the aperture of the microscope. To make certain that our DMD chip would reflect the beam onto the optical axis of the microscope, DMD chip should make a 24 degree angle with optical axis.
10. Tube lens and objective: There is a tube lens inside the microscope and its focal length is 200mm. The beam goes through the tube lens. The collimated illumination beam passes first through the tube lens and then it is refocused by the objective. The objective was

an infinity corrected Nikon 40X objective with working distance of 2.1 mm. The beam hits the surface of the sample and was reflected back.

11. Camera: The beam reflected from the sample after passing through the exit pupil the objective is Collimated. Then it hits a beam splitter that was inside the microscope and passes through a plano-convex lens. I put the camera at the focal plane of the lens to have the real images on the camera.

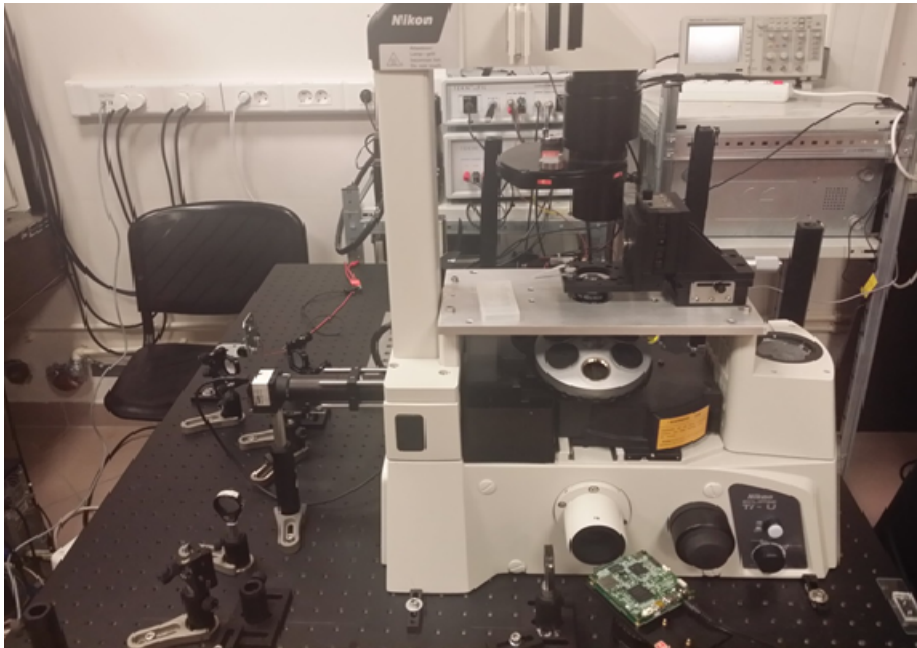


Figure 4.9: The side view of the DMD based microscope optical setup.

4.6 DLP Graphic User Interface (GUI)

To Control the DMD chip, Texas Instruments provided a software. Using this GUI and a mini USB 2 cable, after selecting the stored pattern mode DLP can be connected to the PC [52]. We have used binary patterns. In a pattern where the pixel is black, it corresponds to an off

mirror(-12 degree) and light is deflected outside of the microscope. On the other hand, if the pixel in the pattern is white it corresponds to an on mirror, so beam is reflected from that mirror to the system and will be focused on the focal plane of the objective. There are other options such as controlling the exposure time and the number of the pattern sequences. For DLP lightCrafter the maximum pattern number is 96 (It can be increased up to 1000 patterns by employing an external memory card, however, there would be synchronizing issue). Moreover, the dimensions of the images should be exactly 608×684 pixels. Figure 4.10 displays the screen shot of the GUI.

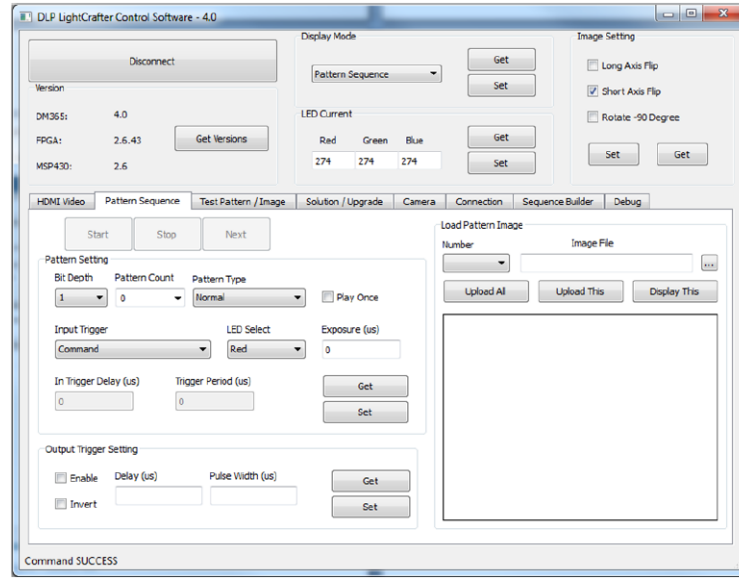


Figure 4.10: Graphic user interface of the DLP LightCrafter EVM.

There is a mini HDMI port on the back side of the DLP chip. By using this port of the DMD and selecting the HDMI mode from the GUI DLP is turned to a projector. Unlike the pattern sequence mode, there is no need to change the screen resolution, the GUI automatically map the screen to 608×684 pixels.

4.7 Scanning Results of the DMD Based Setup

We have used two modes of the DLP module pattern sequences mode and projection mode(see the next section). First we uploaded the pattern sequences to the DLP then obtained images from focal plane of the objective with the CMOS camera. Then using the DLP chip in the HDMI mode and projecting a movie to the focal plane of the objective.

4.7.1 Projection of the Images and pattern sequences by the use of DMD into focal plane of the objective

After construction of the setup the next task was creating some pattern sequences and projecting them on the sample by using the DMD. The dimension of patterns must be 608×684 pixels to be uploaded on the DMD. After choosing the stored pattern mode, uploading the patterns then adjusting the exposure time, we projected patterns on the sample and detected the images with the camera. We started with simple patterns and then with more complex images. The following figures displays the original and projected images:

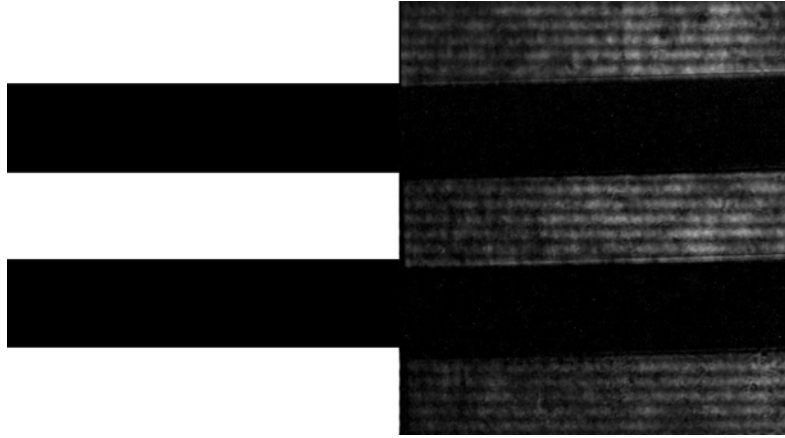


Figure 4.11: A uploaded and the projected pattern on the focal plane of the objective.



Figure 4.12: Original pattern and projected pattern of "Kiraz Lab" on the focal plane of the objective.

4.7.2 Movie projection

Afterwards, we utilized HDMI port of the DMD and projected a movie on the image plane of the objective. For scanning a sample we had to use many patterns and it was possible to do that by putting all of patterns together in a movie and project the movie on the sample for parallel scanning. However, there would be a synchronization trade-off. I have used the HDMI port of the DLP chip to project a movie [53] on the sample.

CHAPTER 5

Appendix

Zemax General Data For the Simulated LSCM Setup

Item	value
Surfaces	29
Stop	5
System Aperture	Entrance Pupil Diameter = 3
Fast Semi-Diameters	on
Field Unpolarized	on
Convert thin film phase to ray equivalent	on
J/E Conversion Method	X Axis Reference
Glass Catalogs	SCHOTT
Ray Aiming	off
Glass Apodization	Uniform, factor = 0.00000E+000
Reference OPD	Exit Pupil
Glass Catalogs	SCHOTT
Paraxial Rays Setting	Ignore Coordinate Breaks
Method to Compute F/#	Pupil Size/Position
Print Coordinate Breaks	on
Multi-Threading	on
OPD Modulo 2 Pi	off
Temperature (C)	2.00000E+001
Pressure (ATM)	1.00000E+000
Adjust Index Data To Environment	Off

Effective Focal Length	1.760702 (in image space)
Back Focal Length	149.3952
Total Track	706.9686
Image Space F/#	0.5869006
Paraxial Working F/#	0.5754808
Working F/#	0.7632484
Image Space NA	0.6485023
Object Space NA	1.5e-010
Stop Radius	1.5
Paraxial Image Height	0
Paraxial Magnification	0
Entrance Pupil Diameter	3
Entrance Pupil Position	200
Exit Pupil Diameter	0.2252256
Exit Pupil Position	0.1317773
Field Type	Angle in degrees
Maximum Radial Field	0
Primary Wavelength [μm]	0.532
Angular Magnification	0
Lens Units	Millimeters
Source Units	Watts
Analysis Units	Watts/ cm^2
Afocal Mode Units	milliradians
MTF Units	cycles/millimeter

Table 5.1: General System Data for LSCM system simulated in Zemax.

Bibliography

- [1] J. B. Pawley, ed., *Handbook Of Biological Confocal Microscopy*. Addison Wesley, third ed., 2006. v, vi, x, 15, 16, 17, 18, 27
- [2] P. Xi, B. Rajwa, J. T. Jones, and J. P. Robinson, “The design and construction of a cost-efficient confocal laser scanning microscope,” *American Journal of Physics*, vol. 75, no. 3, p. 203, 2007. v, vi
- [3] R. H. Webb, “Confocal optical microscopy,” *Reports on Progress in Physics*, vol. 59, no. 3, pp. 427–471, 1999. v, vi, 15
- [4] micro.magnet.fsu.edu/primer/museum/images/janssen.jpg. x, 2
- [5] T. S. Tkaczyk, *Field Guide to Microscopy*. SPIE, 2010. x, 2, 4, 5, 6, 8, 23
- [6] M. T. l. <http://www.olympusmicro.com/primer/anatomy/tubelength.html>. x, 4, 5
- [7] J. M. Geary, *Intoduction to Lens Design, with praxtical Zemax examples*. Willmann.Bell,Inc, 2002. x, xiii, 6, 7, 44
- [8] W. J. Smith, *Modern Optical Engineering*. McGraw-Hill, fourth ed., 2008. x, 7, 10, 13
- [9] <http://wiiphysics.site88.net/images/triangulation.jpg>. x, 12
- [10] http://www.kasalis.com/images/technologies/field_view.png. x, 12
- [11] <http://malone.bioquant.uni-heidelberg.de/methods/imaging/CLSM1.png>. x, 17
- [12] x, 18
- [13] R. L. Price and W. G. J. Jerome, *Basic Confocal Microscopy*. Springer, 2011. x, 3, 19, 20, 21, 24, 34

- [14] www.thorlabs.de, *Amplified Photomultiplier Tube User Guide*. 2012. x, 27
- [15] www.thorlabs.de, *Scan Lenses for Laser Scanning Microscopy*. xi, xiii, 29, 31
- [16] http://www.crestopt.com/optical_handbook/images/fig37.jpg. xi, 30
- [17] “Introduction to Digital Micromirror Device (DMD) Technology,” *Texas Instruments*, 2013. xi, 54
- [18] www.optics.rochester.edu/workgroups/cml/opt307/spr05/john/index_files/image048.jpg. xii, 55
- [19] “DLP LightCrafter Evaluation Module (EVM) User’s Guide,” *Texas Instruments*, 2014. xii, 55, 56
- [20] “Inside the light engine of the DLP LightCrafter EVM,” e2e.ti.com/support/dlp_mems-micro-electro-mechanical_systems/f/850/t/162664. xii, 56, 57
- [21] www.thorlabs.de, *CMOS Cameras*. xiii, 33
- [22] W. J. Croft, *Under The Microscope, a borief history of microscopy*. World Scientific Publishing Co. Pte. Ltd., 2006. 1
- [23] R. Hooke, *Micrographia*. www.gutenberg.net, March 2009. 1
- [24] Britanica Encyclopedia, *Antonie-van-Leeuwenhoek*. 09 2015. Retrieved on 10/09/2015 from <http://global.britannica.com/biography/Antonie-van-Leeuwenhoek>. 1
- [25] M. W. Murphy, Douglas B. and Davidson, *Fundamentals of Light Microscopy and Electronic Imaging*. Wiley-Liss, 2nd ed., 2001. 1, 2, 13
- [26] G. Seward, *Optical Design of Microscopes*. SPIE, 2010. 2, 11
- [27] S. A. van Tendeloo, D. van Dyck, J. van Landuyt, and Gustaaf, eds., *Handbook of Microscopy: Applications in materials Science, Solid-State Physics and Chemistry Methods I*. Addison Wesley, 1997. 2
- [28] http://www.nobelprize.org/nobel_prizes/physics/laureates/1953/. 2

- [29] F. Zernike, “How I discovered phase contrast,” *Science*, vol. 121, pp. 345–349, 1959. 2
- [30] S. M. Wilson and A. Bacic, “Preparation of plant cells for transmission electron microscopy to optimize immunogold labeling of carbohydrate and protein epitopes,” *Nature Protocols*, vol. 7, no. 9, pp. 1716–1727, 2012. 3
- [31] E. Hecht, *Optics*. Addison Wesley, 2001. 4
- [32] R. E. Fischer, B. Tadic-Galeb, and P. R. Yoder, *Optical System Design*. McGraw-Hill, 2008. 7
- [33] Editorial, “Beyond the diffraction limit,” *Nature Protocols*, vol. 3, no. 9, 2009. 9
- [34] N. M. <https://www.microscopyu.com/articles/formulas/formulasna.html>. 10
- [35] <http://www.edmundoptics.com>, *Understanding Microscopes and Objectives*. Retrieved on 06/09/2015 from <http://www.edmundoptics.com/technical-resources-center/microscopy/understanding-microscopes-and-objectives/>. 13
- [36] S. W. Paddock, “Principles and practices of laser scanning confocal microscopy,” *Molecular biotechnology*, vol. 16, no. 2, pp. 127–149, 2000. 15
- [37] www.camtech.com, *6210H Optical Scanner Data sheet*. 27
- [38] G. F. Marshall, *Handbook of Optical and Laser Scanning*. Marcel Dekker, Inc, 2004. 28
- [39] R. E. Hopkins, “Optical System Requirements, For Laser Scanning systems,” 1987. 28
- [40] R. B. Kingslake, Rudolf and Johnson, *Lens Design Fundamentals*. SPIE, seconde ed., 2010. 44
- [41] D. Hill, “How to Optimize on MTF,” 2005. 45
- [42] M. Nicholson, “How to Optimize on MTF,” 2007. 48
- [43] “DLP LightCrafter 4500 Evaluation Module,” *Texas Instruments*, 2014. 55

- [44] L. J. Hornbeck, “Current status and future applications for DMD-based projection displays, Proceedings of the fifth International Display ,” *Workshop IDW 98, Kobe, Japan*, p. 713–716, 1998. 55
- [45] F. Bitte, G. Dussler, and T. Pfeifer, “3D micro-inspection goes DMD,” *Optics and Lasers in Engineering*, vol. 36, pp. 155–167, 2001. 55
- [46] T. Fukano and A. Miyawaki, “Whole-field fluorescence microscope with digital micromirror device: imaging of biological samples,” *Applied optics*, vol. 42, no. 19, pp. 4119–4124, 2003. 55
- [47] C. Maurer, A. Jesacher, S. Bernet, and M. Ritsch-Marte, “What spatial light modulators can do for optical microscopy,” *Laser & Photonics Reviews*, vol. 5, no. 1, pp. 81–101, 2011. 55
- [48] M. Liang, R. L. Stehr, and a. W. Krause, “Confocal pattern period in multiple-aperture confocal imaging systems with coherent illumination,” *Optics letters*, vol. 22, no. 11, pp. 751–753, 1997. 55
- [49] P. KÁŽízek, I. Raška, and G. M. Hagen, “Flexible structured illumination microscope with a programmable illumination array,” *Optics Express*, vol. 20, no. 22, p. 24585, 2012. 55
- [50] D. Dan, M. Lei, B. Yao, W. Wang, M. Winterhalder, A. Zumbusch, Y. Qi, L. Xia, S. Yan, Y. Yang, P. Gao, T. Ye, and W. Zhao, “DMD-based LED-illumination super-resolution and optical sectioning microscopy,” *Scientific reports*, vol. 3, p. 1116, 2013. 55
- [51] E. L. Botvinick, F. Li, S. Cha, D. a. Gough, Y. Fainman, and J. H. Price, “In-vivo confocal microscopy based on the Texas Instruments digital micromirror device,” *Proc. SPIE 3921, Optical Diagnostics of Living Cells III*, vol. 3921, pp. 12–19, 2000. 57
- [52] “Creating Multiple Bit Depth and Multiple Color Pattern Sequences for DLP LightCrafter Kit,” *Texas Instruments, Application Report*, 2013. 62
- [53] <https://www.youtube.com/watch?v=jIMihpDmBpY>. 65

